



NASA  
Contractor Report 191182

Army Research Laboratory  
Contractor Report ARL-CR-81

# Computer Program for Analysis of High Speed, Single Row, Angular Contact, Spherical Roller Bearing, SASHBEAN Volume II: Mathematical Formulation and Analysis

Arun K. Aggarwal  
*Emerson Power Transmission Corporation  
McGill Manufacturing Company  
Valparaiso, Indiana*

DTIC  
ELECTE  
FEB 25 1994  
S C D

September 1993

DISTRIBUTION STATEMENT A

Approved for public release;  
Distribution Unlimited

Prepared for  
Lewis Research Center  
Under Contract NAS3-25423

DTIC QUALITY ASSURED 4

**NASA**  
National Aeronautics and  
Space Administration

94-06047



U.S. ARMY  
**ARL**  
RESEARCH LABORATORY

94 2 24 010

## TABLE OF CONTENTS

### SECTION

PREFACE.....	3
LIST OF SYMBOLS.....	4
1.0 INTRODUCTION.....	8
2.0 FORMULATION OF MATHEMATICAL MODEL.....	9
3.0 LOAD DISTRIBUTION ANALYSIS.....	10
3.1 COORDINATE SYSTEM AND SIGN CONVENTION.....	10
3.2 CONTACT LOAD-DEFORMATION RELATIONSHIP.....	12
3.3 INITIAL CLEARANCES BETWEEN ROLLER-RACEWAY LAMINAE.....	12
3.4 THE ITERATIVE SOLUTION.....	14
4.0 CONTACT STRESS ANALYSIS.....	18
4.1 MAXIMUM AND MEAN CONTACT STRESSES.....	18
4.2 STRESS CONCENTRATION DUE TO EDGE LOADING.....	20
4.3 CONTACT ELLIPSE DIMENSIONS.....	20
4.4 MAXIMUM SUB-SURFACE SHEAR STRESS AND DEPTH.....	20
4.5 ROLLER NORMAL LOADS AND OPERATING CONTACT ANGLES.....	22
5.0 EHD ANALYSIS.....	23
6.0 FATIGUE LIFE ESTIMATION.....	24
6.1 LIFE ADJUSTMENT FACTOR FOR LUBRICATION.....	25
6.2 LIFE ADJUSTMENT FACTOR FOR CONSTRUCTION MATERIAL.....	26

7.0	INTERNAL MOTIONS AND SPEEDS.....	27
7.1	CAGE ROTATION SPEED.....	27
7.2	ROLLER ROTATION SPEEDS.....	29
8.0	RELATIVE SLIDING AT CONCENTRATED CONTACTS.....	31
8.1	INNER RACEWAY CONTACTS.....	31
8.2	OUTER RACEWAY CONTACTS.....	31
9.0	HEAT GENERATION IN THE BEARING.....	32
9.1	DUE TO RELATIVE SLIDING AT CONCENTRATED CONTACTS.....	32
9.2	TRACTION COEFFICIENT UNDER EHD CONDITIONS.....	32
9.3	SLIDING FRICTION AT CAGE GUIDING RAILS/LANDS.....	33
9.4	VISCOUS FRICTION TORQUE DUE TO LUBRICANT.....	34
10.0	THERMAL ANALYSIS.....	35
10.1	METHOD OF HEAT TRANSFER ANALYSIS.....	35
10.2	STEADY-STATE ANALYSIS.....	37
10.3	TRANSIENT ANALYSIS.....	38
11.0	REFERENCES.....	40

## APPENDIX

A	VOLUME OF A FULLY CROWNED SPHERICAL ROLLER.....	43
B	MOMENTS OF INERTIA OF A SPHERICAL ROLLER.....	45
C	INITIAL ESTIMATION OF INTERNAL ROTATIONAL SPEEDS.....	46
D	ROLLER GYROSCOPIC MOTION ANALYSIS.....	47
E	LOAD-DEFORMATION RELATIONSHIP AND MATERIAL FACTORS.....	49

## PREFACE

This report is the second of the two volume documentation for the bearing analysis computer program SASHBEAN. This volume, Volume II, provides the details of the underlying mathematical formulation, analysis, and solution algorithms used for this computer program. A separate volume, Volume I, provides the detailed instructions required to successfully install and effectively use the software for the design and analysis of single row, angular contact, spherical roller bearings.

All efforts involved in the development of this software and its documentation were performed by McGill Manufacturing, Emerson Power Transmission Corporation. This work was done as part of the Advanced Rotorcraft Transmission (ART) Program to advance the state-of-the-art in helicopter transmissions. The ART program was funded by the U.S. Army Aviation Systems Command (AVSCOM) and managed cooperatively by the AVSCOM Propulsion Directorate and the NASA Mechanical Systems Technology Branch, both located at the NASA Lewis Research Center, Cleveland, Ohio. This work was done under a sub-contract to Sikorsky Aircraft Division of United Technologies Corporation, the prime contractor, under NASA contract NAS3-25423.

Technical direction for this project was provided by Sikorsky Aircraft's representatives Mr. C.H. Keller, Jr. and Mr. J.G. Kish, the Task Manager of the project. The government's technical representatives for this work were Dr. R.C. Bill, ART Program Manager and Mr. T.L. Krantz, Project Manager for the Sikorsky ART contract.

The activities performed at McGill Manufacturing were directed by Mr. D.M. Michaels, Project Manager for the sub-contracted project. Analytical and technical support was provided by Mr. J.S. Porter, Mr. R.H. Barber, Mr. C.A. Kruse, Mr. G.A. Satkamp, Mr. A.K. Aggarwal and Mr. W.D. Nutt. Drawing and drafting aid were provided by Mr. D. Wisch and Mr. T. Peterson. Typing and word processing were done by Ms. C. Dodrill and Ms. B. Richards.

Accession For	
NTIS CRA&I	<input checked="checked" type="checkbox"/>
DTIC TAB	<input type="checkbox"/>
Unannounced	<input type="checkbox"/>
Justification	
By	
Distribution/	
Availability Codes	
Dist	Avail and/or Special
A-1	

## LIST OF SYMBOLS

### Alphabets

a	=	Semi-major axis of the contact ellipse (in)
$\bar{A}$	=	Dimensionless material parameter for EHD analysis
b	=	Semi-minor axis of the contact ellipse (in)
c	=	Specific heat of a material (Btu/lbm.°F)
C	=	Initial clearance between a roller-raceway laminae (in)
CF	=	Centrifugal force acting on each roller (lb)
d	=	Distance (in)
dc	=	Diametral clearance (in)
D	=	Roller diameter, maximum (in)
E	=	Young's modulus of elasticity (psi)
$\bar{E}$	=	Equivalent modulus of elasticity (psi)
e	=	Poisson's ratio of a material
F	=	External load on the bearing (radial/axial) (lb)
f	=	Friction force at a sliding contact (lb)
GM	=	Gyroscopic moment acting on each roller (in-lb)
h	=	EHD film thickness, minimum (in)
H	=	Rate of heat generation (Btu/hr)
$I_x$	=	Moment of Inertia of a roller about it's longitudinal axis (in-lb sec <sup>2</sup> )
$I_y$	=	Moment of Inertia of a roller about it's transverse axis (in-lb sec <sup>2</sup> )
$I_z$	=	
i	=	Ring ID; i = 1 for inner; i = 2 for outer
j	=	Roller ID; 1 ≤ j ≤ Z
l	=	Lamina ID; 1 ≤ l ≤ T
K	=	Material constant in the load-deformation relationship for a lamina contact

$L$  = Roller length (in)  
 $L_{-10}$  =  $L_{-10}$  life of a raceway (million revolutions)  
 $LP$  = Lubricant parameter of the lubricant (sec)  
 $M$  = Total pitching moment acting on a roller (in-lb)  
 $N$  = Rotational speed of the bearing (rpm)  
 $\bar{n}$  = Total number of loaded laminae at a raceway  
 $p$  = Mass density of a material (lbm/in<sup>3</sup>)  
 $P$  = Resultant roller load (radial/axial) (lb)  
 $P_e$  = "Equivalent" roller load at a roller-raceway contact (lb)  
 $P_m$  = "Mean" raceway load for all rollers (lb)  
 $P_C$  = Basic dynamic capacity of a raceway (lb)  
 $Q$  = Normal load at a lamina contact (lb)  
 $q$  = Normal load per unit length for a line contact (lb)  
 $r$  = Radius of curvature of the contacting surface (positive for a convex surface, negative for a concave surface)  
 $R$  = Crown radius of roller or raceway  
 $S$  = Contact stress (psi)  
 $t$  = Time (sec)  
 $T$  = Viscous torque of the lubricating fluid (in-lb)  
 $U$  = Mean entrainment velocity (in/sec)  
 $\bar{U}$  = Dimensionless speed parameter for EHD analysis  
 $v$  = Tangential velocity of a rotating point (in/sec)  
 $W$  = Total width of cage rails (in)  
 $w$  = Width of each lamina (in)  
 $\bar{y}$  = Dimensionless load parameter for EHD analysis  
 $Z$  = Total number of rollers in the bearing

### Greek Letters

$\phi$	=	Roller azimuth angle (radians), $0 \leq \phi \leq 2\pi$
$\tau$	=	Shear stress (psi)
$\Gamma$	=	Total number of lamina for a roller
$\delta$	=	Normal approach at a line contact (in)
$\Phi$	=	Ring deflection, relative (in)
$\alpha$	=	Roller angular displacement (pitching) (in/in)
$\beta$	=	Initial contact angle of the bearing (radians)
$\beta'$	=	Operating contact angle of a lamina at the raceway (radians)
$\theta$	=	$D \cos \beta / R$ (bearing geometry parameter)
$\epsilon$	=	Roller deflection (radial/axial) (in)
$n_k$	=	Kinematic viscosity of the lubricant (cStokes) (@ operating temperature and atmospheric pressure)
$n_a$	=	Absolute viscosity of the lubricant (lb.sec/in <sup>2</sup> ) (@ operating temperature and atmospheric pressure)
$\sigma$	=	Surface finish, RMS (in)
$\sqrt{\phantom{x}}$	=	Lubrication film parameter from EHD analysis
$\Omega$	=	Angular velocity of rotation (rad/sec)
$\mu$	=	Coefficient of sliding friction

### Special Characters

$\alpha$	=	Weibull slope
$K$	=	Material factor in the load-deformation relationship for a line contact
$\zeta$	=	Pressure-Viscosity coeff. of the lubricant (in <sup>2</sup> /lb)

$P_t$  = Pitch diameter of the bearing (in)  
 $f$  = Basic dynamic capacity reduction factor  
in fatigue life equation  
 $Y$  = Empirical factor based on bearing type and it's  
lubrication system.  
 $f$  = Indicates functional relationship

### Subscripts

$a$  = Axial direction  
 $brg$  = For the complete bearing  
 $c$  = Composite  
 $cg$  = For cage/retainer  
 $cr$  = For cage rails  
 $eff$  = Effective  
 $fl$  = For lubricating fluid  
 $i$  = Ring number;  $i = 1$  for inner,  $i = 2$  for outer  
 $j$  = Roller number;  $1 \leq j \leq Z$   
 $l$  = Lamina number;  $1 \leq l \leq L$   
 $m$  = Roller mid-plane  
 $max$  = Maximum value  
 $mean$  = Mean value  
 $min$  = Minimum value  
 $o$  = Any roller  
 $r$  = Radial direction  
 $tr$  = Transition point



## 1.0 INTRODUCTION

Spherical roller bearings, known for their high load carrying capacity along with their ability to perform under conditions of misalignments and shaft deflections, have conventionally been restricted to "low" to "moderate" speed applications. Speeds to the order of 5000 rpm or 0.25 million DN have typically [17] been considered as the upper limits for this class of bearings.

The higher coefficient of friction exhibited by a spherical roller bearing, as compared to that of an "equivalent" size cylindrical roller bearing, has been one of the main deterrents for the former's use in high speed applications. In these bearings, the close conformity of roller and raceway spherical crowns, while lending the bearing its self-aligning and high load capacity, also results in relative sliding at the concentrated contacts, resulting in the higher overall coefficients of rolling friction for the bearing.

New concepts in materials, manufacturing techniques, lubricants, component design and design tools are causing revolutions in bearing performance, and spherical roller bearings are no exception. Spherical roller bearings are now being designed and developed for high load and/or high speed applications including aerospace applications.

One such design has been developed by McGill Manufacturing, under a sub-contract from Sikorsky Aircraft Company, as part of an ARMY/NASA sponsored ART project. The bearing, approaching 1.15 million DN, has been tested under full load and full speed conditions.

The trend towards lightweight, high speed, and high performance applications, with increased requirements of reliability and safety, has also placed a great deal of emphasis on the ability to accurately analyze and predict the performance of any suggested design. Such rigorous bearing analysis is no longer restricted by the availability of main frame and mini computers. With the phenomenal development in the power and speed of desk top personal computers, such detailed analysis is now practical on personal computers.

The McGill computer program, SASHBEAN, based on the mathematical formulation described in this report, provides a sophisticated analytical tool to design, analyze, and predict the operating characteristics of single row, angular contact (including zero degree contact angle) spherical roller bearings under high speed conditions.

## 2.0 FORMULATION OF MATHEMATICAL MODEL

To simulate the dynamic performance characteristics of a bearing, the mechanics of internal motions, load and stress distributions, lubricant flow, sliding friction, and heat generation have to be modeled mathematically and solved for the given parameters of bearing geometry, material, empirical factors, and external load and speed environment.

When the bearings involved are of special design, incorporating non-conventional materials, and operating under extreme conditions, these mathematical models, with few simplifying assumptions, no longer allow hand calculations. Computer programs running on high speed digital computers and employing efficient numerical solution techniques are often required to solve such complex mathematical models.

The mathematical model that forms the basis of the computer program SASHBEAN is described in detail in the following sections.

### 3.0 LOAD DISTRIBUTION ANALYSIS

As in any bearing analysis, a major effort involves modeling and solving for the bearing's load distribution among its rolling elements for the given load and speed environment. The loading of the rings at many rolling elements poses a statically indeterminate problem and is often complicated to solve. The problem is further complicated when the high speed dynamic loads on the rolling elements, namely centrifugal forces and gyroscopic moments, are not negligible and are fully considered.

A method, referred to here as the "LAMINA" method, has been employed to solve for the load distribution in the bearing under the combined environment of externally applied loads and high speed dynamic forces. In this technique the roller is divided into a number of slices (laminae), the slicing planes being normal to the roller axis. Similarly each raceway is also considered to be made up of an equal number of laminae. As the deformation at any concentrated contact is very small, it is further assumed that the inter-facial shear between a loaded lamina and an adjoining non-loaded lamina is negligible and that the loaded lamina deforms independently of the non-loaded one under normal loading.

#### 3.1 COORDINATE SYSTEM AND SIGN CONVENTION

Consider a single row, (non-zero) angular contact spherical roller bearing as shown in Figure 1. Let the outer ring be stationary and the inner ring rotating for this formulation. In a real life situation, if the outer was rotating or both inner and outer were rotating, the same formulation will hold as the roller dynamic loads are estimated based on the actual rotational speed of the two rings.

The rollers are numbered 1 through Z sequentially in the clockwise direction and equally spaced, as shown. The azimuth (angular) location of roller #1 is considered as 0.0 degrees and the same increases in the clockwise direction with the roller number. Therefore, the azimuth angle,  $\phi$ , of any roller, j, is given by,

$$\phi_j = 2\pi(j-1)/Z, \quad 1 \leq j \leq Z \quad (3.1)$$

Let the radial load on the bearing be acting along the Y-axis, with roller #1 being directly under the load as shown in Figure 1. The relative radial deflection of the rings is thus positive along the positive direction of the radial load.

An axial load, applied either at the inner or outer ring, is positive when the two rings are pressed into each other. Accordingly, the relative axial deflection of rings is positive when

this deflection causes the rings to move axially towards each other. An axial deflection causing the rings to move away from each other, from the zero end-play position, is thus in the negative direction. A positive axial load, acting along the X-axis is also shown in Figure 1.

Due to the self-aligning ability of a spherical roller bearing, any external moment loading, if present, is not considered.

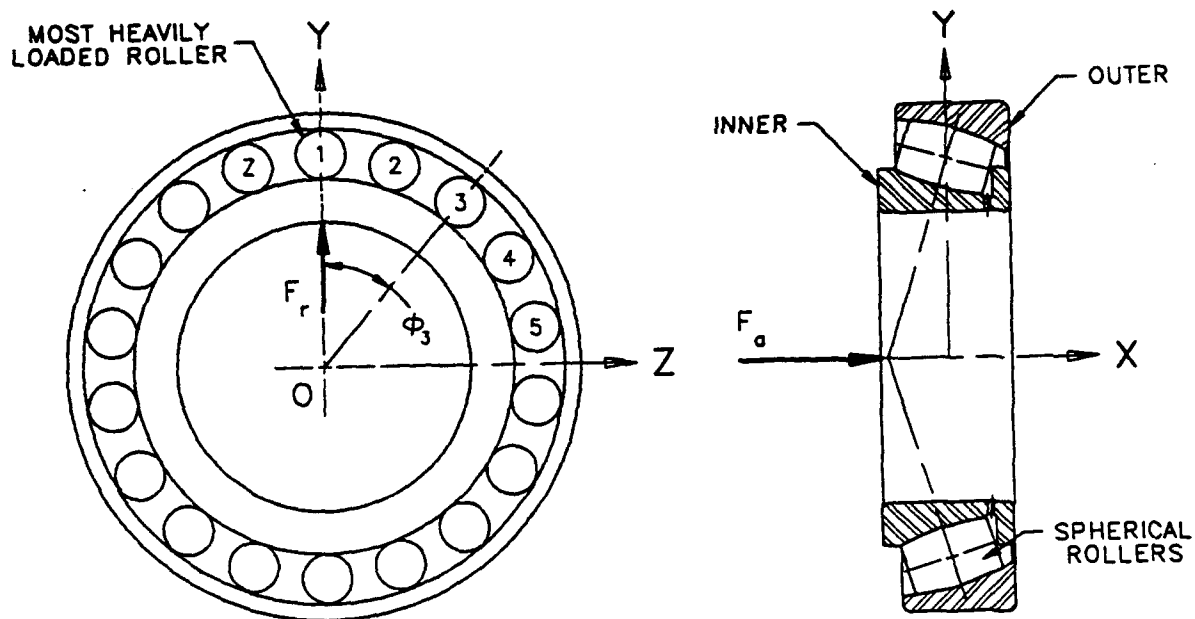


FIGURE 1

### 3.2 CONTACT LOAD-DEFORMATION RELATIONSHIP

For a cylindrical body of finite length,  $L$ , when pressed on to a plane surfaced body of infinite extension, the normal approach,  $\delta$ , between the axis of the cylinder and a distant point in the supporting body is approximately given by,

$$\delta = 4.36E-7[\mathbb{K}^{2.7}q^{.9}L^{.1}] \quad (3.2)$$

where  $\mathbb{K}$  is a factor based on the materials of the two contacting bodies and  $q$  is the normal force per unit length of the contacting cylinder. Appendix E describes in detail the computations for the material factors for different contacting materials.

If the effective length,  $L_{eff}$ , of the roller is subdivided (sliced) in  $\Gamma$  laminae (slices), each of width  $w$ , then equation (3.2) can be rewritten as,

$$\delta = 4.36E-7[\mathbb{K}^{2.7}q^{.9}(\Gamma w)^{.1}]$$

or

$$Q = \frac{(\delta^{1.11}w^{.89})}{(K\Gamma^{.11})} \quad (3.3)$$

where  $K = (4.36E-7\mathbb{K}^{2.7})^{1.11}$  is another constant and  $Q = q.w$  is the total normal force at a lamina contact.

### 3.3 INITIAL CLEARANCES BETWEEN ROLLER-RACEWAY LAMINAE

Due to the difference in the radii of curvatures of roller and raceway crown profiles, there exists varying initial clearances between the roller and raceway laminae. When the bearing is loaded, the contact of a roller lamina,  $l$ , with that of a raceway lamina takes place only after this initial clearance is removed. Figure 2 shows the relative position of a roller,  $j$ , with respect to the two raceways when the bearing is held together with zero radial and axial deflection of the rings. As the roller is subdivided into  $\Gamma$  lamina, each of width  $w$ , the initial clearances at any lamina,  $l$ , can be determined from geometry as follows,

$$C_{i,l} = R_o - (R_o^2 - d_l^2)^{1/2} - [R_i - (R_i^2 - d_l^2)^{1/2}], \quad 1 \leq l \leq \Gamma \quad \& \quad i=1,2 \quad (3.4)$$

Where  $d_l = w(l-l_m)$  is the distance of the lamina,  $l$ , from the roller mid-plane,  $l_m$  being the roller's mid-lamina.

Having established the contact load-deformation relationship and the initial clearances present between the roller and raceway laminae, the load distribution analysis then reduces to determining the relative axial and radial deflections of the rings when in equilibrium under the externally applied loads and the internal forces. For these ring deflections, each roller has to be in

operating equilibrium under the contact forces at raceways and the dynamic loads.

As the loading of the rings at the many rolling element points poses a statically indeterminate problem, further complicated by the inclusion of the dynamic loads in the model, an iterative solution scheme has been deployed to solve this load distribution problem.

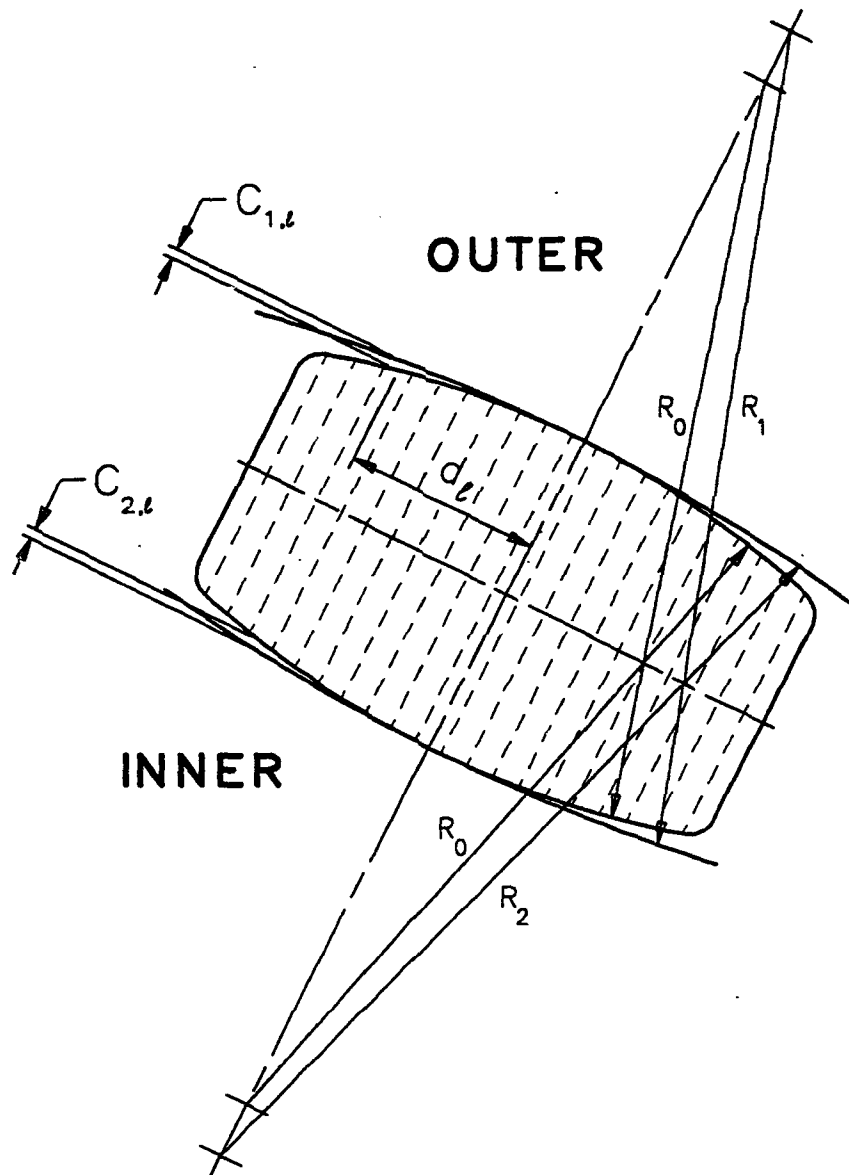


FIGURE 2

### 3.4 THE ITERATIVE SOLUTION

The bearing rings are assigned a small but known set of relative radial and axial deflections. Let these deflections be  $\phi_a$  and  $\phi_r$  respectively. For the given ring deflections,  $\phi_a$  and  $\phi_r$ , we then determine the radial, axial, and angular deflections of each roller by satisfying its equilibrium under radial, axial forces and pitching (misaligning) moments. This is also done using an iterative scheme as described below.

A roller,  $j$ , at azimuth  $\phi$  is assigned a given set of axial, radial and angular displacements as shown in Figure 3. Let  $\alpha$ ,  $\epsilon_a$ , and  $\epsilon_r$  be this roller's angular, axial, and radial displacements respectively. From geometry, for the given ring and roller displacements, we can now write expressions for the normal approach at each lamina as represented below,

$$\delta_{i,j,l} = f(\text{Geometry}, \phi_a, \phi_r \cos \phi, \epsilon_a, \epsilon_r, \alpha) - C_{i,l} \quad (3.5)$$

where  $C_{i,l}$  is the initial clearance at this lamina contact.

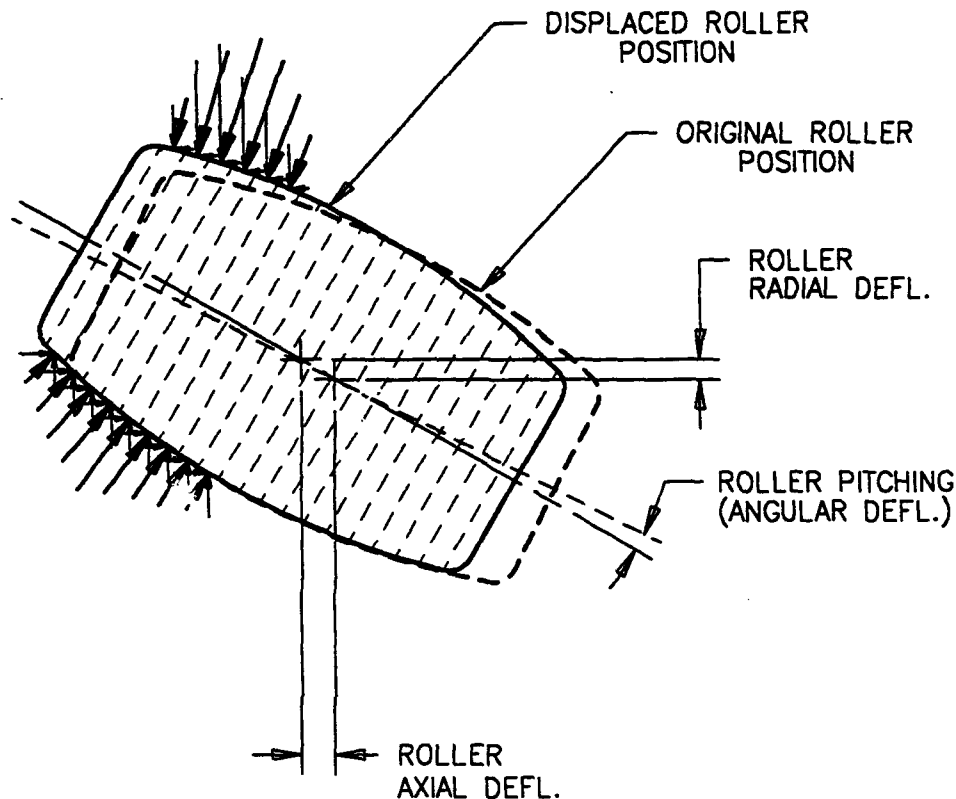


FIGURE 3

A positive and non-zero  $\delta_{i,j,1}$  then indicates a loaded lamina contact. If  $\bar{n}_{1,j}$  and  $\bar{n}_{2,j}$  are the number of loaded laminae, for the roller,  $j$ , at the inner and outer respectively, we can set up the roller equilibrium equations in the axial, radial, and angular directions as follows:

For the equilibrium of this roller in the axial direction,

$$P_{a,i,j} = \frac{w^{.89}}{K\bar{n}_{i,j}^{.11}} \sum_{l=1}^{\bar{n}} \delta_{i,j,l}^{1.11} \cos \beta_{i,j,l} \quad (3.6)$$

For the equilibrium of this roller in the radial direction,

$$P_{r,i,j} = \frac{w^{.89}}{K\bar{n}_{i,j}^{.11}} \sum_{l=1}^{\bar{n}} \delta_{i,j,l}^{1.11} \sin \beta_{i,j,l} \quad (3.7)$$

For the equilibrium of this roller in the angular direction,

$$M_{i,j} = \frac{w^{.89}}{K\bar{n}_{i,j}^{.11}} \sum_{l=1}^{\bar{n}} \delta_{i,j,l}^{1.11} d_l \quad (3.8)$$

Where  $\beta_{i,j,1}$  is the contact angle at the raceway,  $i$ , roller,  $j$ , and lamina,  $1$ .

With the contact forces and moments now known for roller,  $j$ , its (dynamic) equilibrium condition is then established as follows:

a. Check equilibrium of this roller in axial direction:

$$\text{IF } |(P_{a,2,j} - P_{a,1,j})| > \text{Allowed Tolerance} \quad (3.9)$$

THEN adjust this roller's axial deflection and start over for this roller.

b. ELSE Check equilibrium of this roller in radial direction:

$$\text{IF } |(P_{r,2,j} - P_{r,1,j}) - CF| > \text{Allowed Tolerance} \quad (3.10)$$

THEN adjust this roller's radial deflection and start over for this roller.

c. ELSE check equilibrium of this roller's pitching moments:

$$\text{IF } |(M_{2,j} + M_{1,j}) - GM| > \text{Allowed Tolerance} \quad (3.11)$$

THEN adjust this roller's angular displacement and start over for this roller.

ELSE the roller,  $j$ , is found to be in equilibrium for the given



axial, radial and angular roller displacements.

This process is then repeated for all rollers in the bearing and their equilibrium positions determined. In actual programming, taking advantage of the bearing symmetry about a plane through the bearing axis, only a part of the actual number of rollers are solved.

With the equilibrium forces for all the rollers in the bearing now known for the assigned ring deflections, the overall bearing equilibrium equations against the externally applied radial and axial loads are then set up as follows,

(a) Check bearing equilibrium in the radial direction:

$$\text{IF } \left| \sum_{j=1}^Z P_{r,1,j} \cos \phi_j - F_r \right| > \text{Allowed Tolerance} \quad (3.12)$$

THEN adjust rings' relative radial displacement and start over a complete new iteration.

(b) ELSE check bearing equilibrium in the axial direction:

$$\text{IF } \left| \sum_{j=1}^Z P_{a,2,j} - F_a \right| > \text{Allowed Tolerance} \quad (3.13)$$

THEN adjust rings' relative axial displacement and start over a complete new iteration.

ELSE equilibrium of the bearing is established under the given loading environment for these ring deflections.

The normal loads and deflections at each lamina contact are thus known for this (equilibrium) state of the bearing.

A graphical representation (flow chart) of the iterative scheme for this load distribution analysis is shown in Figure 4.

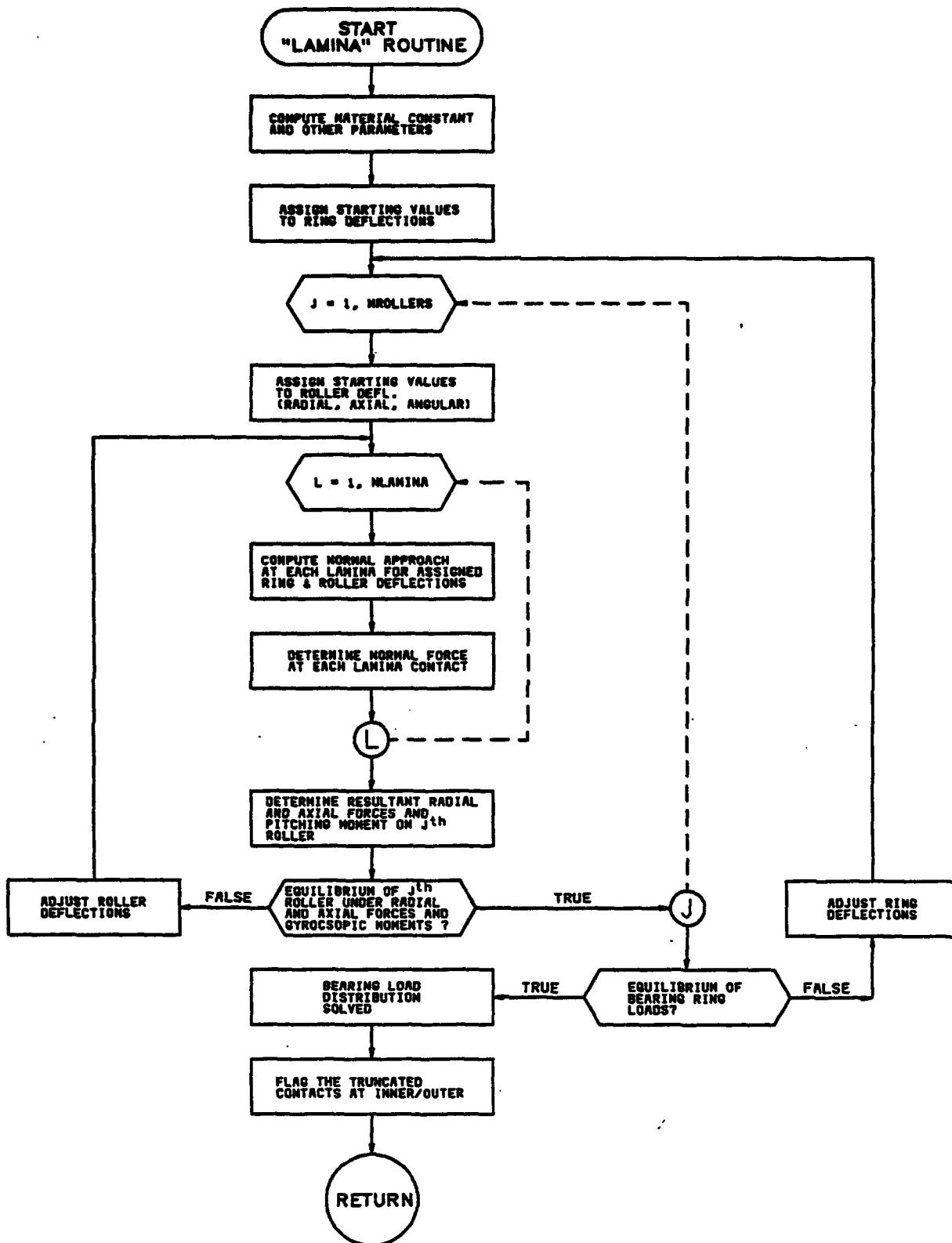


FIGURE 4

## 4.0 CONTACT STRESS ANALYSIS

### 4.0 MAXIMUM AND MEAN CONTACT STRESSES

Having determined the normal forces at each lamina contact, both at inner and outer raceways, the level of contact stresses and areas are then estimated. The simplified formulation of Hertz contact stress analysis for line contacts has been used. The roller and the raceway laminae (slices) are considered as two cylinders of equal length (lamina width), pressed against each other under a known normal load. As the contact deformation at any lamina contact is very small compared to the overall body dimensions, the laminae interface shear is assumed to be negligibly small and thus neglected. A typical arrangement of two parallel cylinders of equal lengths pressed against each other under a normal force is shown in Figure 5. The half width of the lamina line contact,  $b$ , as shown in Figure 5, is given by,

$$b_i = \left[ \frac{Q(\hat{e}_o + \hat{e}_i)}{\pi w(r_o^{-1} + r_i^{-1})} \right]^{\frac{1}{2}} \quad (4.1)$$

where  $\hat{e}_o$  and  $\hat{e}_i$  are elastic constants of the two bodies based on the respective values of modulus of elasticity and Poisson's ratio of their materials.  $r_o$  and  $r_i$  are the radii (with proper signs as per sign convention) of the roller and raceway laminae respectively as shown in Figure 5. The maximum and mean contact stresses are then given by,

$$S_{\max} = (2Q) / (\pi w b) \quad (4.2)$$

$$S_{\text{mean}} = (Q) / (2wb) = \pi S_{\max} / 4 \quad (4.3)$$

In the computer program, the contact width, maximum and mean contact stresses are computed at each lamina contact. The maximum of maximum and the maximum of mean contact stresses of all the loaded lamina of the roller,  $j$ , at the inner raceway are taken as this roller's maximum and mean contact stresses at the inner contact.

Similarly, the maximum and mean contact stresses of this roller at the outer contact are given by the maximum of maximum and the maximum of mean lamina stresses at the outer contacts.

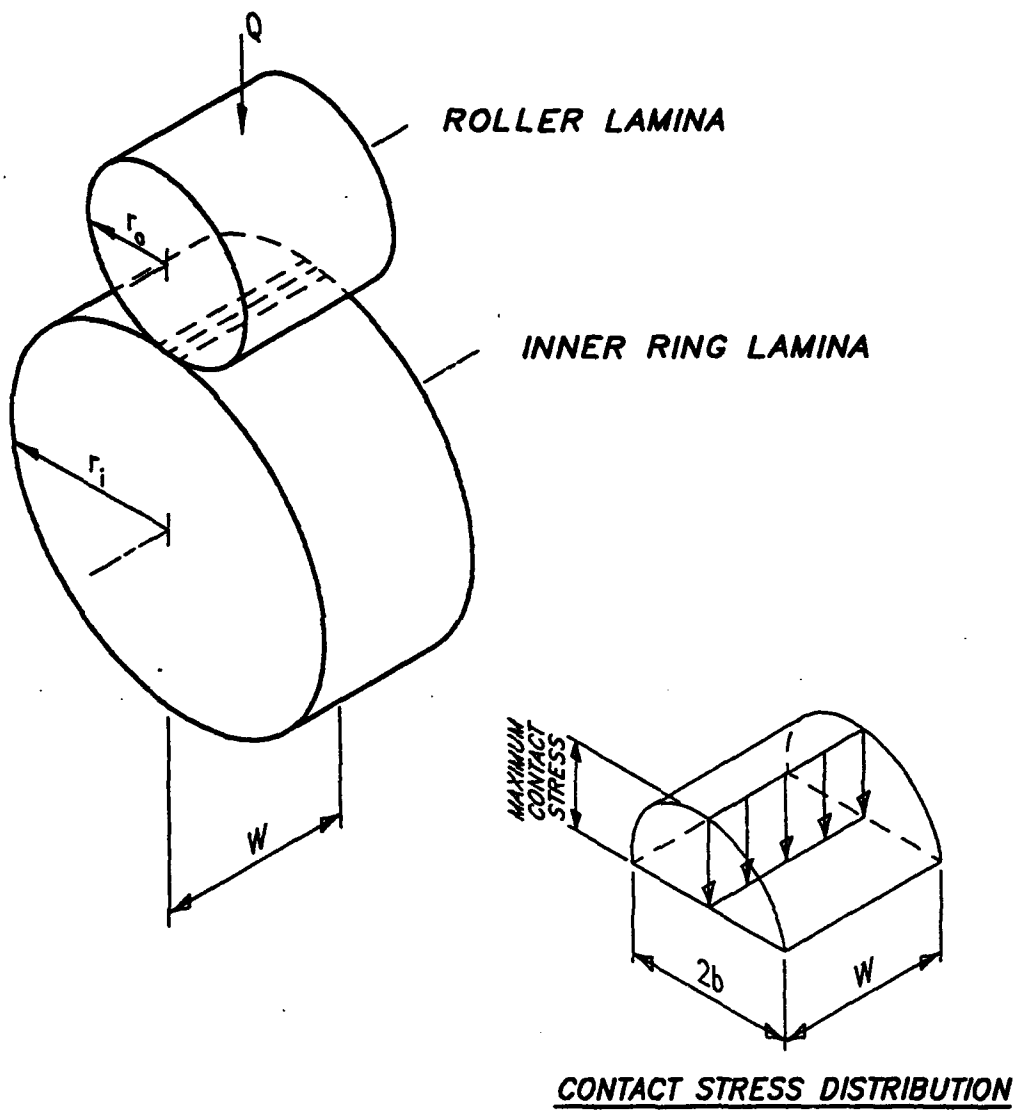


FIGURE 5

#### 4.2 STRESS CONCENTRATION DUE TO EDGE LOADING

If for a roller, any of its "edge" laminae are in contact with the raceway and thus loaded, its (roller's) contact ellipse may not be fully contained on its effective length and is truncated at the loaded edge. Due to stress concentration, the level of contact pressure at such edge laminae is thus expected to be higher than that calculated by the above Hertz analysis.

A user specified stress concentration factor is thus applied (multiplied) to these edge laminae normal loads. Accordingly, the calculated Hertz contact stresses at these laminae contacts also get adjusted by this stress concentration factor. Factors of the order of 1.5 - 2.0 are typically used.

After applying the stress concentration factors, the maximum of maximum and the maximum of mean laminae contact stresses for each roller both at the inner and outer raceways, are also printed out in the program output file.

#### 4.3 CONTACT ELLIPSE DIMENSIONS

Cumulative width of the loaded laminae of a roller at the inner contacts gives us the major axis of the roller's contact ellipse at this raceway. The width of the line contact at the most heavily loaded lamina of this roller at the same raceway gives us the minor axis of the contact ellipse.

The axial distance of the most heavily loaded lamina mid-plane from the roller mid-plane, being called as the eccentricity of the contact ellipse, is also computed and written out for each roller.

The contact ellipse major axis, minor axis, and eccentricity for each roller at the outer raceway contacts are also determined in a similar fashion and printed out.

#### 4.4 MAXIMUM SUB-SURFACE SHEAR STRESS AND DEPTH

As the material below a concentrated contact is also in a state of stress and the rolling contact fatigue failures have been known to originate from these subsurface points, the magnitude and depth of this subsurface shear stress is also of importance to a bearing analyst.

By considering the stresses caused by the normal contact load and further application of the principles of elasticity theory, Jones [11] has presented the expressions for the three principal stresses occurring at a point along the Z-axis, any depth below the contact surface as shown in Figure 6.

Since the surface contact pressure is maximum along the Z-axis, the three principal stresses must also attain their maximum values along the same axis. The maximum shear stress is then given by half of the maximum difference between any two principal stresses. The depth of this point (of maximum shear stress) can also be determined.

For simplicity, the graphical method suggested by Jones [11] has been used for these estimations. The graph presented in reference [11], as shown in Figure 7, gives the maximum shear stress and its depth of occurrence as a function of contact ellipse dimensions ratio  $b/a$ .

With the contact ellipse dimensions and the maximum contact pressure known for each roller-raceway contact, the maximum sub-surface shear stress and its depth, are directly read from the graph of Figure 7, in the computer program. For a complete discussion on this topic and the derivation of underlying equations, the reader is referred to Jones [11] and Harris [9].

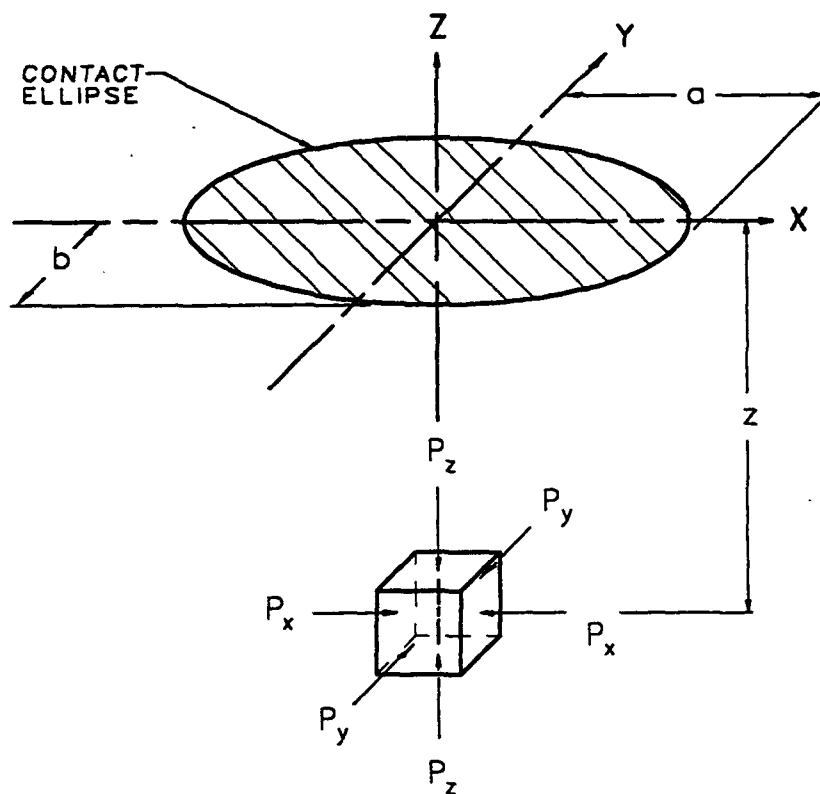


FIGURE 6

## MAXIMUM SUB-SURFACE SHEAR STRESS/DEPTH FROM REFERENCE [11]

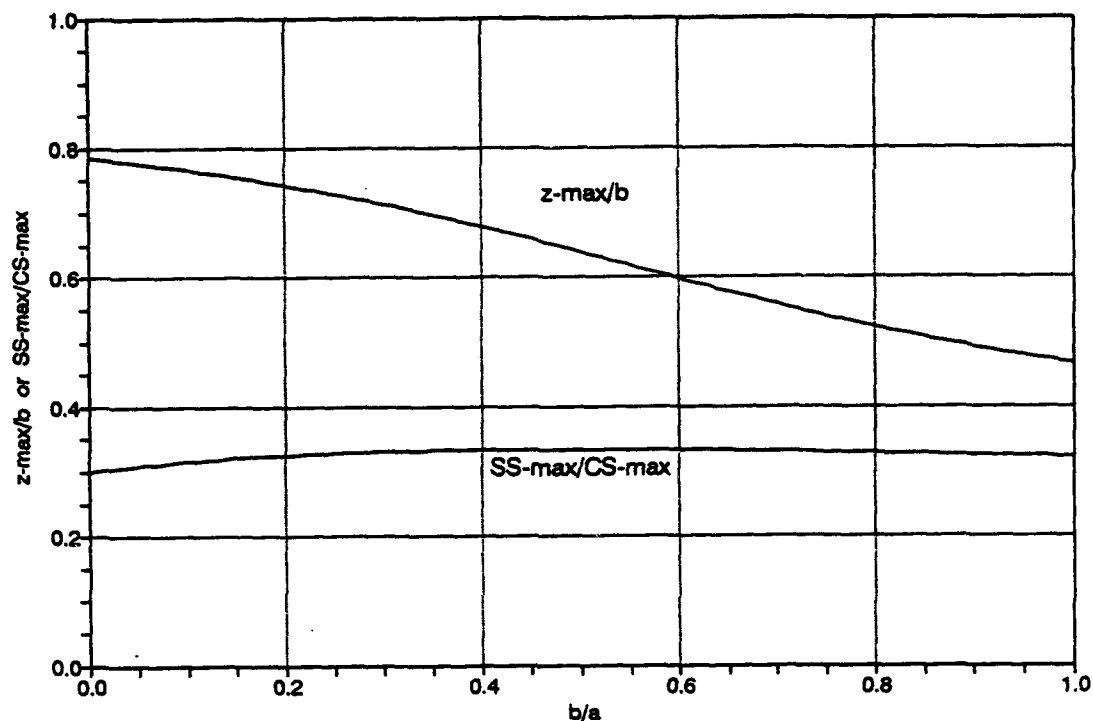


FIGURE 7

### 4.5 ROLLER NORMAL LOADS AND OPERATING CONTACT ANGLES

The contact angle of the most heavily loaded lamina of a roller at the inner is taken as the operating contact angle of this roller at the inner raceway. Similarly, the contact angle of the most heavily loaded lamina of this roller at the outer is taken as the operating contact angle of this roller at the outer raceway.

The summation of the components of a roller lamina loads at the inner contacts, along the contact angle of the most heavily loaded lamina at this raceway, gives the roller-inner contact normal load for this roller. Similarly, the roller-outer normal load for this roller is given by the summation of lamina load components along the contact angle of the most heavily loaded lamina at the outer.

## 5.0 EHD ANALYSIS

Grubin's equation [23] has been used for EHD film thickness estimation at each lamina contact. This is due to the fact that the ASME recommended life adjustment curve for EHD lubrication is also based on computations using the same equation as given below:

$$h_{\min} = 1.95 R_{eq} (\bar{U})^{8/11} (\bar{A})^{8/11} (\bar{Y})^{-1/11} \quad (5.1)$$

where,

$h_{\min}$  = Minimum thickness of the EHD film (in)

$R_{eq} = (R_1 R_0) / (R_1 \pm R_0)$  is the "equivalent" radius of the two contacting surfaces. The plus sign is for external contacts (both surfaces convex) and minus for the internal contacts (surface with larger radius of curvature is concave)

$\bar{U} = (n_a U) / (\bar{E} R_{eq})$  is the dimensionless speed parameter

$\bar{A} = (\bar{c} \bar{E})$  is the dimensionless material parameter

$\bar{Y} = Q / (\bar{E} R_{eq} w)$  is the dimensionless load parameter

$U = \frac{1}{2}(U_o + U_i)$  is the mean entrainment velocity (in/sec)

$\bar{E} = \frac{1}{2} \left[ \frac{1 - e_o^2}{E_o} + \frac{1 - e_i^2}{E_i} \right]$  is the "equivalent" modulus of elasticity (psi)

Rewriting (5.1) with definitions of various parameters, we get,

$$h_{\min} = 1.95 R_{eq} (n_a \bar{c} U / R_{eq})^{8/11} (Q / \bar{E} R_{eq} w)^{-1/11} \quad (5.2)$$

Furthermore, in equation (5.2) the two lubricant properties,  $n_a$  and  $\bar{c}$  can be combined into one parameter, known as Lubricant Parameter (LP), as defined below,

$$LP = 10^{11} n_a \bar{c} \quad (5.3)$$

This Parameter combines both pressure and temperature-viscosity characteristics of the lubricant and thus contains lubricant's entire contribution to the formation of EHD film. Mobil, for example, publishes this data for their premium lubricating oils.

Lubricant properties in the above formulation are expected at the temperature of contacting surfaces at the EHD film inlet region. As the oil film is very thin, it is believed that it quickly attains the inlet surface temperature. If this surface temperature is unknown and cannot be easily determined, the oil outlet temperature or the average of the inlet and outlet temperatures may be used as a good approximation.



## 6.0 FATIGUE LIFE ESTIMATION

A method, referred to here as "Equivalent Roller Loads" method, has been used for the estimation of raceways' L-10 fatigue lives. In this method, the nonuniform and skewed load distribution along the roller length, as expected in high speed spherical roller bearings, is accounted for by first calculating what is being termed as "Equivalent" roller loads. These are computed from the roller's individual lamina loads at a raceway using the product law of probability.

According to this law, the probability of survival of the entire raceway is the product of the probabilities of survival of each individual lamina (slice). Using the roller "Equivalent" loads at a raceway then allows the use of formulation developed for estimating the L-10 fatigue life of a roller-raceway under radial load with line contact. Harris [9] describes in detail the derivations for the equation used and presented here for calculating the roller "Equivalent" loads, from the known normal lamina loads,  $Q_{i,j,l}$ , as follows:

$$P_{e,i,j} = r^{7/9} \left[ \sum_{l=1}^{l=r} Q_{i,j,l}^{9/2} \right]^{2/9} \quad (6.1)$$

$P_e$  being the "equivalent" roller-raceway normal contact load at raceway,  $i$ , and roller,  $j$ ,. The fatigue lives of inner and outer raceway are then given by,

$$L-10 = (P_c/P_m)^4 \text{ million revolutions}$$

Where  $P_c$  is the Basic Dynamic capacity of the raceway and  $P_m$  is the "mean" roller load at this raceway.  $P_c$  for inner and outer raceways are given by,

$$P_{c,1} = 49500(\xi) \frac{(1-\theta)^{29/27}}{(1+\theta)^{1/4}} \left[ \frac{\theta}{\cos \beta} \right]^{2/9} (D)^{29/27} (L_{eff})^{7/9} (Z)^{-1/4} \quad (6.2a)$$

$$P_{c,2} = 49500(\xi) \frac{(1+\theta)^{29/27}}{(1-\theta)^{1/4}} \left[ \frac{\theta}{\cos \beta} \right]^{2/9} (D)^{29/27} (L_{eff})^{7/9} (Z)^{-1/4} \quad (6.2b)$$

Where equation (6.2a) is for the inner and equation (6.2b) is for the outer raceway.  $\xi$  is a Bearing Dynamic Capacity reduction factor based on the bearing type and is a user input to the program. Typically, for angular contact spherical roller bearings,  $\xi$  lies between 0.60 and 0.85.

The "mean" roller-raceway load,  $P_m$ , is the quartic mean of the roller "equivalent" loads at this raceway and is given by,

$$P_{m,i} = \left[ \frac{1}{Z} \sum_{j=1}^Z P_{e,i,j}^4 \right]^{1/4} \quad \text{for the rotating raceway} \quad (6.3)$$

$$P_{m,i} = \left[ \frac{1}{Z} \sum_{j=1}^Z P_{e,i,j}^{4\alpha} \right]^{1/4\alpha} \quad \text{for the stationary raceway} \quad (6.4)$$

The L-10 fatigue lives of the raceways are then given by,

$$L-10_i = (P_{c,i}/P_{m,i})^4 ; \quad i = 1, 2 \quad (6.5)$$

The L-10 fatigue life of the complete bearing may then be determined using the law of probability as follows,

$$L-10_{brg} = (L-10_1^{-\alpha} + L-10_2^{-\alpha})^{-1/\alpha} \quad (6.6)$$

In the computer program, the overall bearing life is computed and printed out, both before and after applying the lubrication and material life adjustment factors to the computed raceway lives.

#### 6.1 LIFE ADJUSTMENT FACTOR FOR LUBRICATION

In the computer program, the  $h_{min}$  is estimated at each concentrated lamina contact using the user specified data on lubricant properties at the expected surface temperatures. The minimum of the minimum EHD film thicknesses at each raceway is then used for calculating the film parameter,  $\sqrt{}$ , at that raceway. The composite rms surface finish of the two surfaces is calculated from their individual rms surface finishes as follows:

$$\sigma_{c,i} = (\sigma_o^2 + \sigma_i^2)^{1/2} ; \quad i = 1, 2 \quad (6.7)$$

The film parameter,  $\sqrt{}$ , for a raceway is then given by,

$$\sqrt{i} = h_{min,i}/\sigma_{c,i} \quad (6.8)$$

The ASME recommended curve for life adjustment factors has been extended for lower values of  $\sqrt{}$  (down to  $\sqrt{=} 0.1$ ) and used for reading the raceway life adjustment factors for lubrication. The extension of the original ASME curve for lower values of  $\sqrt{}$  is based on the collected test and field data from Sikorsky. This extended ASME curve has been coded into the computer program using cubic splines interpolation and is shown in Figure 8.

## LUBRICATION LIFE ADJUSTMENT FACTORS (ASME CURVE EXTENDED FOR LOWER LAMBDA S)

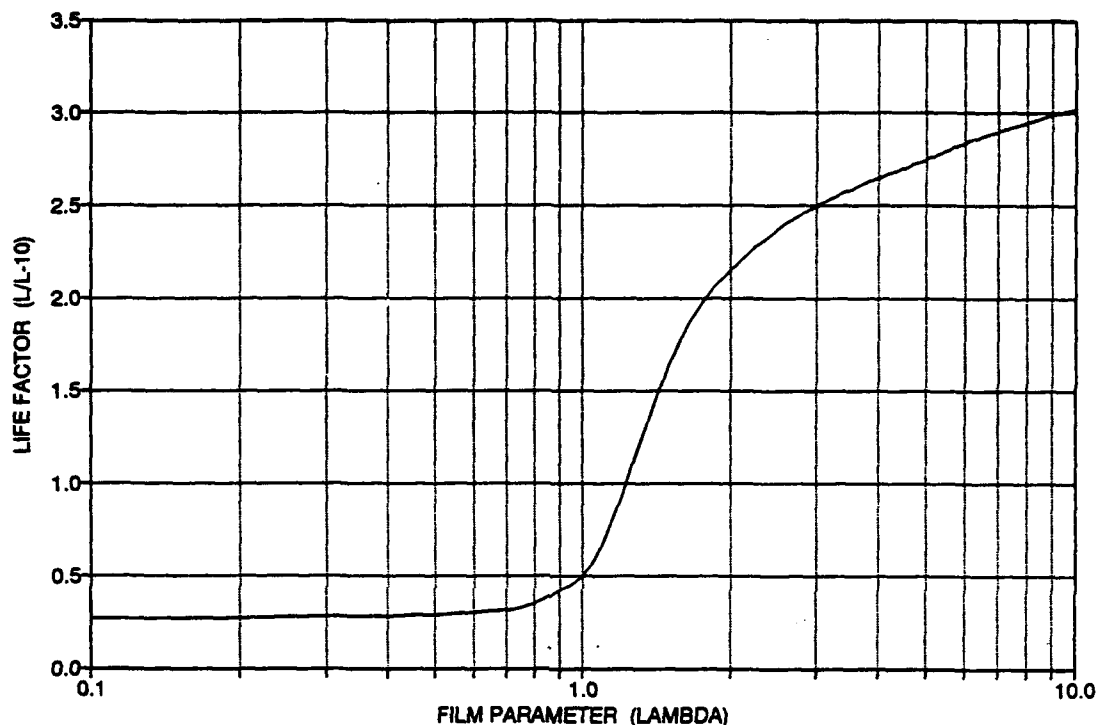


FIGURE 8

For  $1 \leq \sqrt{\lambda} \leq 10$  the life adjustment factor,  $L/L-10$ , is returned as per the curve shown in figure 8. For  $\sqrt{\lambda} < 0.1$ , a value of 0.27 is returned and for  $\sqrt{\lambda} > 10$ ,  $L/L-10$  factor of 3.02 is returned. The computer program prints out both the estimated and adjusted raceways and bearing lives in the program output file.

### 6.2 LIFE ADJUSTMENT FACTOR FOR CONSTRUCTION MATERIAL

An appropriate life adjustment factor, based on the construction material of the bearing components, is supplied by the program user. This factor is directly multiplied to the calculated L-10 lives of the bearing raceways along with the life adjustment factors due to lubrication. The adjusted raceway lives are then used in equation (6.6) to estimate the adjusted bearing life.

## 7.0 INTERNAL MOTIONS AND SPEEDS

With the operating equilibrium position of each roller in the bearing now known, the average cage and roller rotation speeds are estimated as described below.

### 7.1 CAGE ROTATION SPEED

Assuming no skidding at the concentrated roller-raceway contacts, the cage tangential velocity is taken as the average of the tangential velocities of the most heavily loaded points of the "controlling" rollers at the inner and outer contacts. The rollers loaded both at the inner and outer raceways are considered as the rollers "controlling" the cage rotation. The rollers loaded only at one raceway are, on the other hand, considered as "controlled" (orbited) by the rotating cage.

Consider the operating position of the roller,  $j$ , at the inner raceway as shown in Figure 9. Let  $A$  be the contact center (most heavily loaded point) and  $r_1$  be the radial distance of point  $A$  from the bearing axis as shown. If  $\beta_1$  is the contact angle of roller,  $j$ , at point  $A$ , then from geometry

$$r_1 = (AP) \cos \beta_1 \quad (7.1)$$

Where  $AP = OP - OA$  is also determined from geometry. The tangential velocity of the point  $A$ , when lying on the inner raceway, is then given by,

$$v_1 = \Omega_1 r_1 \quad (7.2)$$

Similarly for the most heavily loaded point  $A$  at the outer raceway contact for this roller, as shown in Figure 10, we can write:

$$r_2 = (AP) \cos \beta_2 \quad (7.3)$$

and

$$v_2 = \Omega_2 r_2 \quad (7.4)$$

Where  $AP$  is now given by  $AP = OP + OA$  and is once again determined from geometry.

Then, for no gross slip, taking the cage tangential velocity due to roller,  $j$ , as the average of the tangential velocities  $v_1$  and  $v_2$  we get,

$$v_{cg} = \frac{1}{2}(v_1 + v_2) = \frac{1}{2}(R\Omega_{cg}) \quad (7.5)$$

The cage rotation speed due to roller,  $j$ , is then given by,

$$\Omega_{cg,j} = (v_1 + v_2)/R \quad (7.6)$$

## ROLLER AT INNER RACEWAY

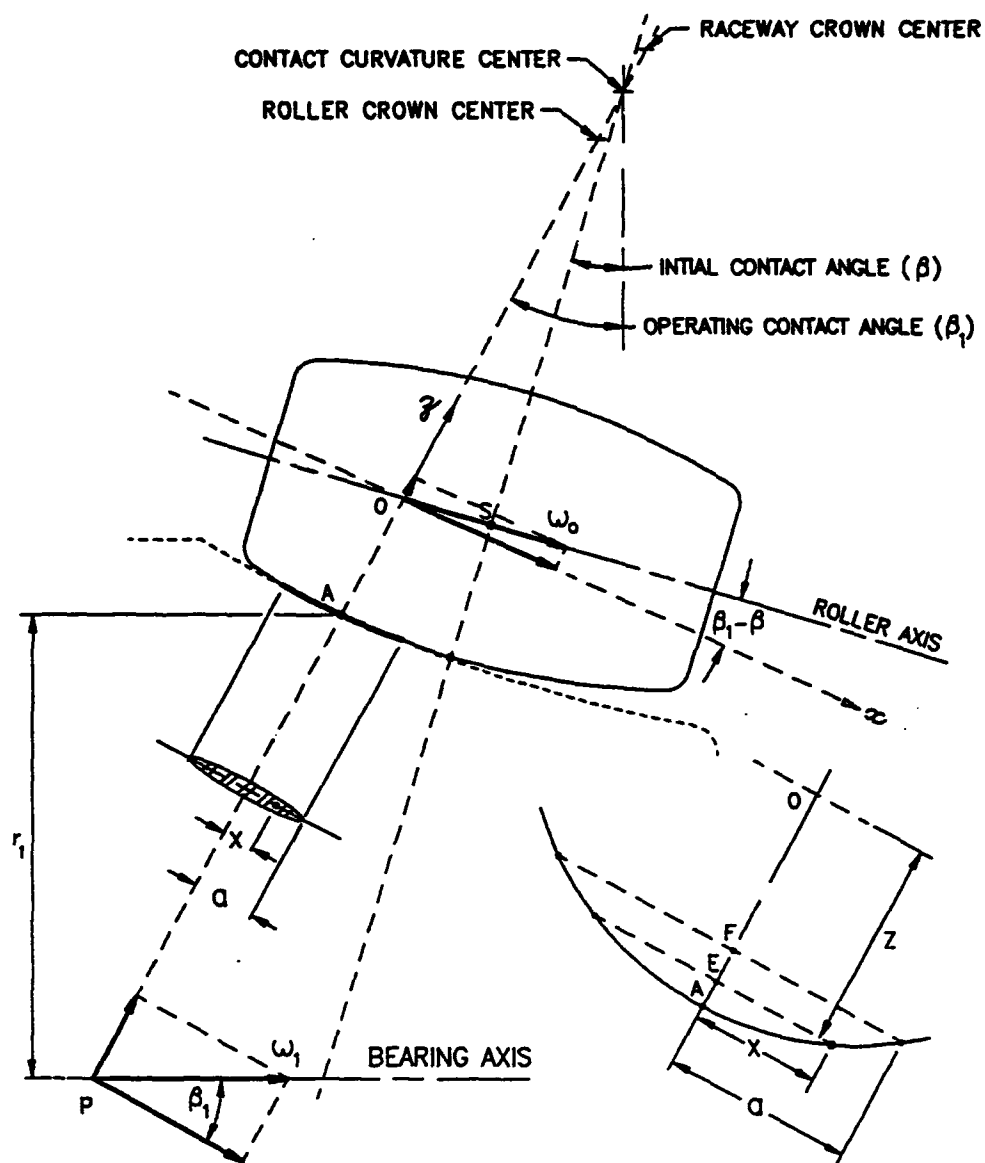


FIGURE 9

If  $Z_{eff}$  is the number of rollers loaded at both raceways, thus controlling the cage rotation, the expected average cage rotation speed is taken as the arithmetic mean of the cage speeds due to each of the controlling rollers as given by,

$$\Omega_{cg} = (\sum_{j=1}^{Z_{eff}} \Omega_{cg,j}) / Z_{eff} \quad (7.7)$$

## 7.2 ROLLER ROTATION SPEEDS

Assuming pure rolling at the most heavily loaded points at the inner and outer contacts, the rotational speed of a roller,  $j$ , is taken as the average of the two speeds imparted to this roller by the two raceways.

Once again considering the contact of a roller,  $j$ , at the inner as shown in Figure 9. The radial distance of point A, the most heavily loaded point, from the roller axis is given by,

$$r_{o,1} = (OA) \cos(\beta_1 - \beta) \quad (7.8)$$

For no slip at this point, the rotational speed of the roller due to the inner raceway contact, is then given by,

$$\Omega_{o,1} r_{o,1} = (\Omega_1 - \Omega_{cg}) r_1 \quad (7.9)$$

Similarly, by considering the contact of the same roller at the outer, as shown in Figure 10, we can write,

$$r_{o,2} = (OA) \cos(\beta - \beta_2) \quad (7.10)$$

and

$$\Omega_{o,2} r_{o,2} = (\Omega_2 - \Omega_{cg}) r_2 \quad (7.11)$$

Where  $\Omega_{o,2}$  is the rotational speed of the  $j^{th}$  roller due to the outer raceway contact.

The average of two roller speeds, due to inner rotation ( $\Omega_{o,1}$ ) and outer rotation ( $\Omega_{o,2}$ ) as given by equations (7.9) and (7.11), gives us a good estimate of the expected roller rotational speed. Therefore, for the roller,  $j$ ,

$$\Omega_o = \frac{1}{2}(\Omega_{o,1} + \Omega_{o,2}) \quad (7.12)$$

This is true for all the rollers loaded at both raceways. For the rollers loaded at one raceway only, the rotational speed is taken as the speed imparted by the contacting raceway, assuming a pure rolling at the most heavily loaded point of this contact.

## ROLLER AT OUTER RACEWAY

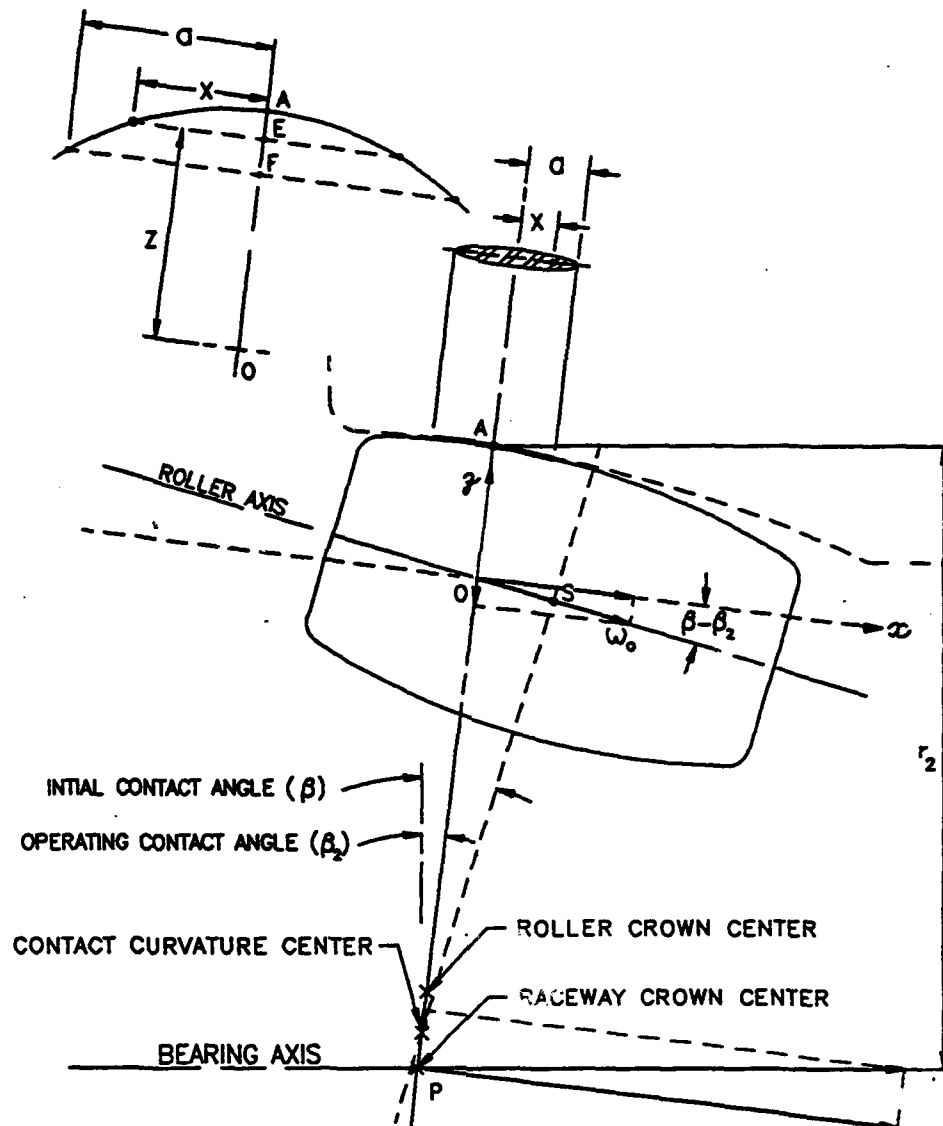


FIGURE 10

## 8.0 RELATIVE SLIDING AT CONCENTRATED CONTACTS

Having determined the rotational speeds of the bearing cage about the bearing axis, and of each roller about its own axis, we can now estimate the magnitude and direction of expected relative sliding at each concentrated contact.

### 8.1 INNER RACEWAY CONTACTS

Let Oxyz be a local coordinate system with origin at O as shown in Figure 9. The y-axis being perpendicular and into the plane of paper. For a point (x,y,z), lying on the contact ellipse of this roller at the inner raceway, the y coordinate is negligible as compared to x and z coordinates. This is due to the fact that the contact ellipse has a high ellipticity, its minor axis being very small compared to its major axis.

Let the point (x,z) on the contact ellipse lie on the inner raceway surface. The tangential velocity of this point along the y-axis is given by,

$$v_1 = -(OP-OE)\Omega_1 \cos\beta_1 + x\Omega_1 \sin\beta_1 \quad (8.1)$$

When the same point (x,z) is considered lying on the roller surface, its tangential velocity along the same axis (y-axis) would be given by,

$$v_o = (OE)\Omega_o \cos(\beta_1 - \beta) + x\Omega_o \sin(\beta_1 - \beta) \quad (8.2)$$

where OP and OE are determined from the known geometry. The relative sliding velocity of this point (x,z) is then given by,

$$v_{rel,1} = v_1 - v_o \quad (8.3)$$

### 8.2 OUTER RACEWAY CONTACTS

Similarly, by considering a point (x,z) on the contact area of a roller at the outer raceway, as shown in Figure 10, we can write the expressions for the tangential velocities of this point when lying on the outer raceway and roller surfaces as follows,

$$v_2 = -(OP+OE)\Omega_2 \cos\beta_2 + x\Omega_2 \sin\beta_2 \quad (8.4)$$

$$v_o = -(OE)\Omega_o \cos(\beta - \beta_2) - x\Omega_o \sin(\beta - \beta_2) \quad (8.5)$$

Relative sliding velocity of this point (x,z) is then given by,

$$v_{rel,2} = v_2 - v_o \quad (8.3)$$



## 9.0 HEAT GENERATION IN THE BEARING

Total heat generation in a spherical roller bearing comes from various friction mechanisms occurring during the bearing operation. These include shear stressing of the EHD oil films due to the relative sliding motion at the concentrated contacts, viscous friction torque of the lubricant against the ploughing motion of the rolling elements through the lubricant, sliding friction at the cage lands and rails. In a high speed bearing of this type, the major contribution to the total heat generation, under normal operating conditions, is due to the sliding friction at the concentrated contacts under EHD conditions.

In the formulation for SASHBEAN computer program, heat generation due to the three mechanisms mentioned above has been considered. These are described in detail in the following sections.

### 9.1 DUE TO RELATIVE SLIDING AT CONCENTRATED CONTACTS

To estimate the traction force at the sliding Elastohydrodynamic contacts, a formulation presented by Allen et. al. [1] has been used.

### 9.2 TRACTION COEFFICIENT UNDER EHD CONDITIONS

As per the above model, four parameters, namely - ambient absolute viscosity, pressure-viscosity coefficient, a lubrication factor (a pseudo coefficient of friction), and a transition shear stress, can quantify the traction in a sliding EHD contact. Mathematically stated, the shear stress for a Newtonian fluid in a concentrated contact under EHD conditions is given by,

$$\tau = [\eta_a \exp(\phi S)] v_{rel} / h_{min} \quad \text{when } \tau < \tau_{tr} \text{ and } \tau < \mu_{fl} S \quad (9.1)$$

$$= \mu_{fl} S \quad \text{when } \tau > \tau_{tr} \text{ and } \tau > \mu_{fl} S \quad (9.2)$$

Where  $S$  is the normal contact pressure at a lamina,  $\tau_{tr}$  being the *transitional* shear stress (typically 1000 psi), and  $\mu_{fl}$  is the lubricant factor - the pseudo coefficient of friction (typically between 0.045 and .075).

Having determined the shear stress ( $\tau$ ) in the EHD film at each lamina contact, the total traction force for the given lamina contact is then evaluated by integrating the shear stress over the entire contact area of this lamina contact.

With the relative sliding velocity at each lamina contact already known, the heat generation due to relative sliding is then given by the thermal equivalent of the mechanical work done against

this friction force.

*Rate of Work Done = Traction Force x Relative Sliding Velocity*

The thermal equivalent of this mechanical work is then taken as the rate of heat generation in the bearing and is given by,

*Rate of Heat Generation = Rate of Work Done/2.5933*

where the factor 2.5933 converts the mechanical work (in-lb/sec) to equivalent heat units (Btu/hr).

To estimate the sliding friction force at the concentrated contacts under lost lubrication conditions, it is assumed that the Newtonian viscosity relationship for the fluid shear stress no longer holds valid. A constant (user supplied) coefficient of traction coefficient is used for evaluating the sliding friction forces, the mechanical work done, and the resulting heat generation at each concentrated contact.

### 9.3 SLIDING FRICTION AT CAGE GUIDING RAILS/LANDS

The Petroff's equation [25], which provides a good approximation for the power loss in lightly loaded journal bearings, has been used to estimate the resisting torque of the lubricant present in the clearances between the ring lands and the cage rails. Following assumptions have been made for this formulation,

- (a) Resultant cage-roller loads are very small.
- (b) Cage is properly balanced and while rotating maintains a uniform gap with the guide ring.
- (c) Radial gap between the ring land(s) and the cage rail(s) is fully flooded with the lubricating fluid.
- (d) Viscosity of the lubricating fluid in the gap does not change appreciably from the bulk of lubricant in bearing cavities.

The tangential friction force at the cage-ring interface is then given by,

$$f_{cr} = \pi (n_a W_{cr} D_{cr} |\Omega_{cg} - \Omega_i|) / (dc_{cr}) \quad (9.3)$$

Where  $i=1$  for an inner guided cage and  $i=2$  for an outer guided cage.  $W_{cr}$  is the total width of the cage rails in sliding contact with the guide ring rails,  $D_{cr}$  is the mean interface diameter,  $\Omega_i$  is the angular velocity of the guiding ring, and  $dc_{cr}$  is the diametral clearance between the guiding ring lands and the cage rails. The resulting heat generation due to this friction power

loss is then given by,

$$H_{cr} = 0.1928(D_{cr}f_{cr}|\Omega_{cg}-\Omega_i|) \quad (9.4)$$

#### 9.4 VISCOUS FRICTION TORQUE DUE TO LUBRICANT

The viscous drag torque, experienced by the rollers moving through the lubricant flooded bearing cavities, has been estimated using the empirical equation suggested by Harris [9] and Eschmann [5] for high speed bearings as presented below,

$$T_{fl} = 1.42E-5Y(n_k N)^{2/3} \mu^3 ; \quad n_k N > 2000 \quad (9.5)$$

Where,

$T_{fL}$  = Viscous friction torque of the lubricating fluid (in-lb)

$Y$  = A factor based on the bearing type and its lubrication system. As per ref. [9],  $Y = 5$  for spherical roller bearings under oil bath lubrication.

The heat generation in the lubricant due to its viscous friction torque is then given by the thermal equivalent of the mechanical work done against this viscous drag. This is given by,

$$H_{fl} = 0.0404(N.T_{fl}) \quad (9.6)$$

where the factor of 0.0404 converts the rate of mechanical work (in-lb./min) to equivalent rate of heat generation (Btu/hr).

## 10.0 THERMAL ANALYSIS

With the amount of heat generation at different points in the bearing now known, thermal models are then set up to perform a steady-state and transient heat transfer analysis. These analyses can predict the expected steady-state and time-transient temperature maps of various points in a bearing system respectively. Some detailed information about the bearing application, including its supporting system, dimensional and material data, lubricant properties, and lubrication system, are required to prepare the model data for thermal analysis.

A steady-state condition would be one when a certain lubricant flow rate is maintained through the bearing system. After an initial "warm up" time, the temperatures at different points of the bearing and its supporting mechanical system would have stabilized and there is no further variation in temperatures at any point throughout the system.

When a "stabilized" system is subjected to a sudden change in environment and its steady-state condition disturbed, the system temperatures would become time variant. One such change of environment could be the loss of lubricant flow through the bearing system. A transient heat transfer analysis would be called for in such a situation to predict the time-temperature history of various points in the system. This information may then be used to predict bearing's time-to-failure in the event of lubrication failure.

### 10.1 METHOD OF HEAT TRANSFER ANALYSIS

A method known as "Lumped-Heat-Capacity" method has been used for modeling and analyzing the system for steady-state and transient temperatures. In this method, the whole system is considered made up of small elements, with the entire thermal capacity of each element "lumped" at its center and assuming a uniform temperature distribution throughout the volume of the element.

In other words, the internal resistance to heat flow within an element is considered negligibly small compared to its external resistance to heat flow from the surface to the surrounding elements. In general, smaller the size of elements, the more realistic these assumptions are for lumped-heat-capacity analysis.

For ease of data preparation, the maximum number of elements for a single bearing system have been limited to 20 in this program. The model prepared for the steady-state and transient thermal analyses of MCGILL SB-1231 and SB-1231-1 bearings is shown in Figure 11. The element and node numbers are marked on the same figure. The lubricating oil circuit is shown by the dotted lines.

# THERMAL ANALYSIS MODEL FOR THE TEST BEARING AND ITS SUPPORTING SYSTEM

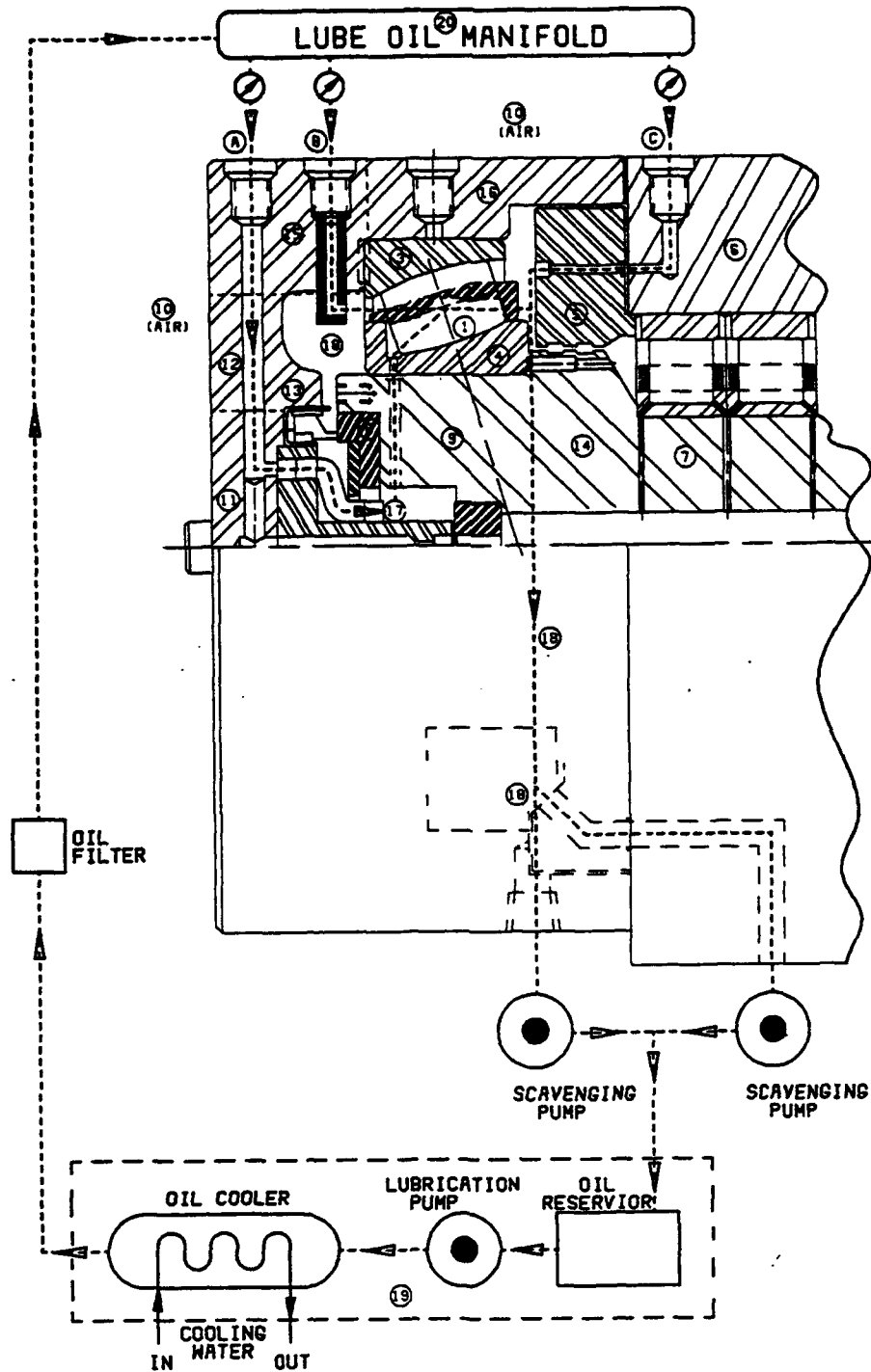


FIGURE 11

## 10.2 STEADY-STATE ANALYSIS

SASHBEAN Computer Program is capable of analyzing and predicting the steady-state temperature map of an axisymmetric mechanical system of any cross-section. The mechanical system is first approximated by an equivalent system comprised of a number of elements of simple geometries. Each element is then represented by a node point and its node number. The temperature at this node point (element) may or may not be known. Heat sources (with known heat generation rates) are assigned to any nodes representing the elements of heat generation within the bearing. The environment surrounding the system, also having heat transfer with the system, is also represented by one or more nodes. As mentioned earlier, a maximum of 20 nodes are allowed by the program to describe the equivalent thermal model.

With the elements and their node points properly selected, the heat balance equations considering different modes of heat transfer are then set up for each node. Heat transfers by conduction, free and forced convection, and mass transfer are considered. Radiation heat transfer, being very small as compared to other modes in such applications, has been neglected.

Now for a steady state condition to exist, the net flow of heat to a node  $i$  from its surrounding nodes  $j$  plus the heat generated at node  $i$  must be equal to zero. This heat balance at node  $i$  results in an algebraic equation with some nodal temperatures as unknowns. As this condition would be true for all the nodes in the system, heat balance condition at each node results in an algebraic equation for that node.

Assuming a linear relationship for free and forced convection modes, the resulting mathematical model is a system of linear algebraic equations with the unknown nodal temperatures as the unknown variables. The analysis then reduces to solving this system of algebraic equations for the unknown variables.

Consider the heat energy flowing into node  $i$  from its surrounding nodes  $j$ . If  $N$  is the total number of nodes in the model, then for the steady state condition to exist,

$$\text{Net heat flowing into node } i = 0$$

or,

$$Q_i + \sum_j^n f_1(T_j - T_i) + f_2(T_j - T_i) + f_3(T_j - T_i) + f_4(T_j - T_i) = 0 \quad (10.1)$$

Where  $f_1$ ,  $f_2$ ,  $f_3$ , and  $f_4$  are the coefficients in respective heat transfer equations for various modes of heat transfer between the elements. Volume I of this documentation, the USER'S GUIDE, provides more details on various modes and their applicable

equations. Rewriting equation (10.1) we get,

$$Q_i = \sum F_{ij} (T_j - T_i) = 0 ; \quad i = 1, n \quad (10.2)$$

where,

$$F_{ij} = f_1 + f_2 + f_3 + f_4 \quad (10.3)$$

Equation (10.2) represents a system of linear algebraic equations for  $1 \leq i \leq N$ . Depending upon the actual number of surrounding nodes  $j$  interacting with node  $i$ , each equation may or may not have all the unknown variables.

For a node (say node  $j$ ) with a given (known) temperature, the heat balance equation for this node is replaced by the equality  $T_j = T_{\text{given}}$  and the unknown variable  $T_j$  substituted for the known,  $T_{\text{given}}$ , in the remaining equations of the system.

The Gauss-Jordan numerical scheme, with partial pivoting, has been deployed to invert the coefficient matrix for the solution of this system. Reference [3] provides a detailed discussion on this and other numerical methods.

### 10.3 TRANSIENT ANALYSIS

The formulation for computing the steady-state temperatures was based on the condition that the net energy transfer into any node,  $i$ , from its surrounding nodes,  $j$ , is zero. Therefore, no further change of element temperatures then took place at this condition.

For the transient formulation, on the other hand, a net energy transfer to the node  $i$  from its surrounding nodes  $j$  takes place resulting in an increase in the internal energy of the element  $i$ . Precluding any phase changes, this increase in the internal energy results in a temperature rise for the element  $i$ . As each element volume is considered to have "lumped" capacity at its node point, the interaction of all the elements thus determines the behavior of the complete system.

For the mathematical formulation of the transient problem, the net heat energy into a node  $i$  from its surrounding node(s)  $j$  in a very small interval of time ( $dt$ ) is equated to the energy required to raise the temperature of the element  $i$  to a new value. Heat transfer by conduction, free and forced convections are considered. To simulate the lost-lubricant condition no heat transport by mass transport of the lubricant is now available. The lubricant nodes in the steady state model are replaced by air nodes having a forced convective heat transfer with the bearing elements.

The resulting equation for the node,  $i$ , is a linear differential

equation of first order with a known initial value. The element's steady-state temperature, estimated prior to this analysis, is used as the initial value at time  $t = 0$ .

If the internal energy of an element,  $i$ , is expressed in terms of its specific heat and temperature, its rate of change with time,  $t$ , is equal to the net heat energy gained by the node,  $i$ , in the small interval of time,  $dt$ . Therefore we can write that,

$$q = \frac{dE_i}{dt} = (c_i p_i v_i) \frac{dT_i}{dt} \quad (10.4)$$

Where  $c$  is the specific heat,  $p$  the mass density, and  $v$  the volume of the element,  $i$ , material. Using an explicit finite difference approximation we can then transform the differential equation (10.4) into a finite difference equation as follows,

$$q = \frac{\Delta(E_i)}{\Delta(t)} = (c_i p_i v_i) \frac{T_i^{P+1} - T_i^P}{\Delta(t)} \quad (10.5)$$

Where  $T_i^P$  and  $T_i^{P+1}$  are the temperatures of element,  $i$ , at time  $t$  and  $t + \Delta(t)$  respectively.

The total heat gain,  $q$ , of this element,  $i$ , from the surrounding elements,  $j$ , in the same time interval,  $\Delta(t)$ , by various modes of heat transfer, is also given by,

$$q = Q_i + \sum_j F_{ij} (T_j^P - T_i^P) \quad (10.6)$$

Therefore by equating (10.5) and (10.6) and solving for  $T_i^{P+1}$  we get,

$$T_i^{P+1} = (Q_i + \sum_j F_{ij} T_j^P) \frac{\Delta(t)}{C_i} + [1 - \frac{\Delta(t)}{C_i} \sum_j F_{ij}] T_i^P \quad (10.7)$$

Where,  $C_i = c_i p_i v_i$  is the thermal capacity of the element  $i$ .

If  $T_i^P$  is known at time  $t$ , then  $T_i^{P+1}$  at time  $t + \Delta(t)$  can be determined from equation (10.7) for the element  $i$ . This process is repeated for each node in the model and this time-marching solution continues till the desired temperature or time limit is reached. As mentioned before, the nodal steady-state temperatures are used as the initial values at time  $t = 0$ .



## 11.0 REFERENCES

1. Allen, C.W., Townsend, D.P., and Zaretsky, E.V., "New Generalized Rheological Model For Lubrication of a Ball Spinning in a Nonconforming Groove", NASA Technical Note # D-7280, May, 1973.
2. Beer, F.P., and Johnson Jr., E.R., "Vector Mechanics for Engineers - Statics and Dynamics", Fifth Edition, McGraw-Hill, 1985.
3. Charpa, S.C. and Canale, R.P., "Numerical Methods For Engineers with Personal Computer Applications", McGraw-Hill, 1985.
4. Coe, H.H., "Thermal Analysis of a Planetary Transmission with Spherical Roller Bearings Operating After Complete Loss of Oil", NASA Technical Paper 2367, Sept. 1984.
5. Eschmann, Hasbargen, and Weigand, "Ball and Roller Bearings - Theory, Design, and Application", Second Edition, Revised by Hasbargen, L. and Brändlein, J., John Wiley and Sons, 1985.
6. Hadden, G.B., Kleckner, R.J., Ragen, M.A., and Sheynin, L., "Research Report and User's Manual for Computer Program SHABERTH", SKF Report No. AT81Y0003, NASA CR-165365, May, 1981.
7. Hamrock, B.J., and Dowson, D., "Ball Bearing Lubrication - The Elastohydrodynamics of Elliptical Contacts", John Wiley and Sons, 1982.
8. Harris, T.A., and Mindel, M.H., "Rolling Elements Bearing Dynamics", Wear, Vol. 23, pp. 311-337, 1973.
9. Harris, T.A., "Roller Bearing Analysis", Second Edition, John Wiley and Sons, 1984.

10. Holman, J.P., "Heat Transfer", Fourth Edition, McGraw-Hill, 1976.
11. Jones, A.B., "Analysis of Stresses and Deflections", New Departure Engineering Data, Bristol, Conn., 1946.
12. Jones, A.B., "The Mathematical Theory of Rolling Element Bearings", Mechanical Design and Systems Handbook, Second Edition, Ed. Rothbart, H.A., pp. 13.1-13.75, McGraw-Hill, 1990.
13. Kahaner, D., Moler C., and Nash, S., "Numerical Methods and Software", Prentice Hall, 1989.
14. Keller Jr., C.H., and Morrison, F.R., "Development of a Thrust-Carrying Cylindrical Roller Bearing for Helicopter Transmissions", Report prepared by Sikorsky Aircraft, Division of United Technologies Corp. under contract from Applied Technology Laboratory, U.S. Army Research and Technology Laboratories (AVRADCOM), Sept. 1980.
15. Kellstrom, E.M., "Rolling Contact Guidance of Rollers in Spherical Roller Bearings", Paper presented at the Joint ASME/ASLE Lubrication Conference, Dayton, Ohio, Oct. 16-18, 1979, ASME Paper #79-LUB-23.
16. Kleckner, R.J., and Dyba, G., "High Speed Spherical Roller Bearing Analysis and Comparison with Experimental Performance", Advanced Power Transmission Technology, NASA Conference Publication 2210, pp. 239-252, 1983.
17. Kleckner, R.J., and Pirvics, J., "Spherical Roller Bearing Analysis. SKF Computer Program SPHEARBEAN. Volume I: Analytic Formulation", SKF Report No. AT81D006, Submitted to NASA/Lewis Research Center, NASA/NTIS Report No. CR-165203, Dec. 1980.

18. Kleckner, R.J., and Dyba, G., "Spherical Roller Bearing Analysis. SKF Computer Program SPHEARBEAN. Volume II: User's Manual", SKF Report No. AT81D007, Submitted to NASA/Lewis Research Center, NASA/NTIS Report No. CR-165204, Dec. 1980.
19. Lundberg, G. and Palmgren, A., "Dynamic Capacity of Rolling Bearings", ACTA POLYTECHNICA, Mech. Eng. Ser. 1, No. 3, Vol. 7, 1947.
20. Lundberg, G. and Palmgren, A., "Dynamic Capacity of Roller Bearings", ACTA POLYTECHNICA, Mech. Eng. Ser. 1, 1952.
21. Mobil Oil Corporation, "Mobil EHL Guidebook", Third Edition, Mobil Technical Publications, 1981.
22. Palmgren, A., "Ball and Roller Bearing Engineering", Second Edition, Translated by Palmgren, G., and Ruley, B., S.H. Burbank and Co. Publisher, Philadelphia, 1946.
23. Skurka, J.C., "Elastohydrodynamic Lubrication of Roller Bearings", Jr. Lubrication Technology, pp. 281-288, April 1970.
24. The Society of Tribologists and Lubrication Engineers, "Starting from Scratch - Tribology Basics", A compilation of articles previously published in Lubrication Engineering, Ed. Fred Litt, STLE, Park Ridge, Illinois.
25. Wilcock, D.F., and Booser, E.R., "Bearing Design and Application", First Edition, McGraw-Hill, 1957.
26. Winer, W.O., and Cheng, H.S., "Film Thickness, Contact Stress and Surface Temperatures", Wear Control Handbook, pp. 81-141.

## APPENDIX - A

### VOLUME OF A FULLY CROWNED SPHERICAL ROLLER

Volume of a spherical roller, required in the estimation of centrifugal force and gyroscopic moment acting on a roller, is determined using simple integral calculus as follows.

- Let OXYZ be a coordinate frame of reference with its origin at the roller center as shown in Figure 12. The coordinates of the roller crown radius center (O') are then given by  $x_0 = 0$  and  $y_0 = -(R_0 - D/2)$ . Therefore, the profile of the roller crown can be represented by the following equation of a circle,

$$(x-x_0)^2 + (y-y_0)^2 = R_0^2 \quad (A.1)$$

or,

$$y = (R_0^2 - x^2)^{1/2} + y_0 \quad (A.2)$$

Now by considering the volume of a roller slice of differential thickness,  $dx$ , at a distance  $x$  from the roller mid-plane (as shown in Figure 12) and integrating it for the full roller length we get,

$$V = \int_L dV = \pi \int_L y^2 dx \quad (A.3)$$

By substituting for  $y = y(x)$  from equation (A.2) into equation (A.3) and integrating w.r.t  $x$  we get an expression for the volume of a fully crowned spherical roller.

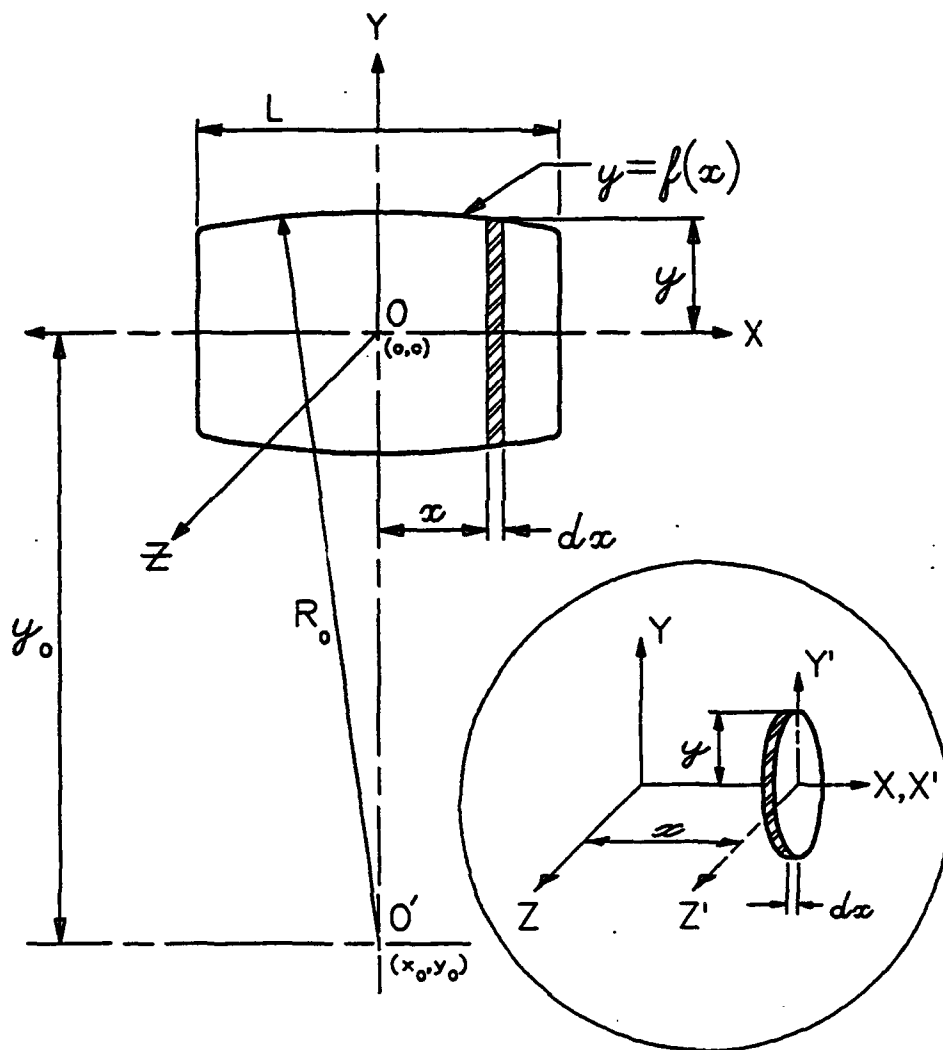


FIGURE 12

## APPENDIX - B

### MOMENTS OF INERTIA OF A SPHERICAL ROLLER

Mass Moments Of Inertia (MMOI) of the roller, both about its longitudinal and transverse axes, are required for the calculations of gyroscopic moment acting on each roller. The expressions for these have also been derived by considering a roller slice of differential thickness and integrating over the full length of a roller, as summarized below.

By referring to Figure 12 and considering the roller slice as shown, the moments of inertia of the slice about the X, Y, and Z axes are given by,

$$dI_X = \frac{1}{2}y^2 dm \quad (B.1)$$

$$dI_Y = dI_{Y_1} + x^2 dm = (\frac{1}{2}y^2 + x^2) dm \quad (B.2)$$

$$dI_Z = dI_{Z_1} + x^2 dm = (\frac{1}{2}y^2 + x^2) dm \quad (B.3)$$

Where  $dI_{Y_1}$  and  $dI_{Z_1}$  are the moments of inertia of the disk about a local coordinate axes  $X'Y'Z'$ , with origin at the disk center and parallel to the global axes  $OXYZ$  as shown in Figure 12.  $dm$  is the mass of the differential disk and is given by,

$$dm = p dv = p \pi y^2 dx \quad (B.4)$$

$p$  being is the mass density of the roller material. Roller's spherical profile is described by  $y = (R_o^2 - x^2)^{\frac{1}{2}} + y_o$  as derived in equation (A.2) of Appendix-A with  $y_o = -(R_o - D/2)$ .

By substituting equation (B.4) into equations (B.1), (B.2), and (B.3) and performing the integration w.r.t.  $x$  for  $x$  varying from  $-L/2$  to  $+L/2$ , we get the expressions for roller's mass moments of inertia about its longitudinal axis ( $I_x$ ) and transverse axes ( $I_y$ ,  $I_z$ ). Due to its symmetry about the X-axis, we get  $I_y = I_z$ .

## APPENDIX - C

### INITIAL ESTIMATION OF INTERNAL ROTATIONAL SPEEDS

To estimate the magnitudes of the roller dynamic loads, namely the centrifugal force and gyroscopic moment, an initial estimate of the cage rotational speed about the bearing axis and each roller's rotational speed about its own longitudinal axis was first made under the following assumptions:

(a) The operating contact angle of each roller is the initial design contact angle of the bearing. In other words, the contact ellipse at each concentrated contact is centered about the roller center.

(b) No gross slip occurs at any concentrated contact.

The tangential velocity of the cage is then given by the mean of the tangential velocities of contact center points at the inner and outer raceways. Thus,

$$\Omega_{cg} = \frac{1}{2}[\Omega_1(1-\theta) + \Omega_2(1+\theta)] \quad (C.1)$$

or,

$$N_{cg} = \frac{1}{2}[N_1(1-\theta) + N_2(1+\theta)] \quad (C.2)$$

The rotational speed of each roller about its own axis, required for estimating the gyroscopic moment on each roller, is then given by,

$$N_o = (R/2D)(1-\theta)(1+\theta)(N_2 - N_1) \quad (C.2)$$

## APPENDIX - D

### ROLLER GYROSCOPIC MOTION ANALYSIS

In angular contact spherical roller bearings, the motion of each roller is very similar to that of a gyroscope. Like a gyroscope rotor, the roller is rotating (gyroscopic spin) about its own geometric axis, unparallel to the bearing axis, and also orbiting (gyroscopic precession) about the bearing axis along with the cage. The gyroscopic moments seen by these rollers, often neglected for low speed and/or low contact angle analyses, become quite significant in high speed applications and considerably affects the roller deflections and load distributions.

The formulation for the SASHBEAN Computer Program takes into full consideration this moment loading of the rollers. The assumptions made for the estimation of the magnitude of this moment acting on each roller are listed below:

- (a) The cage has a constant angular velocity of rotation about its (or bearing) axis as determined in Appendix C.
- (b) Each roller has the same constant angular velocity about its longitudinal axis as determined in Appendix C.
- (c) The roller misalignment (pitching) angle at any azimuth location is negligibly small when compared to the design contact angle of the bearing.
- (d) The operating contact angle of each roller is the same as the design contact angle of the bearing.

Consider a roller at any angular location ( $\phi$ ) as shown in Figure 13. Let OXYZ be a fixed frame of reference with its origin, O, at the intersection of bearing and roller axes. Let o'xyz be a rotating system of axes, attached to the roller with origin at the roller mass center as shown in the same figure. By considering the roller as a gyroscopic rotor we can see that for this gyroscope,

$$\text{Nutation Angle} = \text{Roller-Raceway Contact Angle} = \beta$$

$$\text{Precession Angular Velocity} = \text{Roller Orbital Velocity} = \Omega_{cg}$$

$$\text{Spin Angular Velocity} = \text{Roller Rotational Velocity} = \Omega_o$$

By considering the special case of the gyroscopic motion where  $\beta$ ,  $\Omega_{cg}$ , and  $\Omega_o$  remain constant, the couple (moment) required on the roller (the rotor) to sustain this motion is given by,

$$GM = [I_z(\Omega_o + \Omega_{cg} \cos \beta) - I_x(\Omega_{cg} \cos \beta)] \Omega_{cg} \sin \beta \quad (D.1)$$



This couple, applied to the roller by the raceways, is about an axis perpendicular to the precession and spin axes of the gyroscope. The moment vector is thus directed along the positive y-axis (perpendicular and pointing into the plane of the paper). The reaction couple of the roller, resisted by the raceways, is equal in magnitude and opposite in direction. For a detailed discussion on the topic and derivation of the above equation, the reader is referred to reference [2].

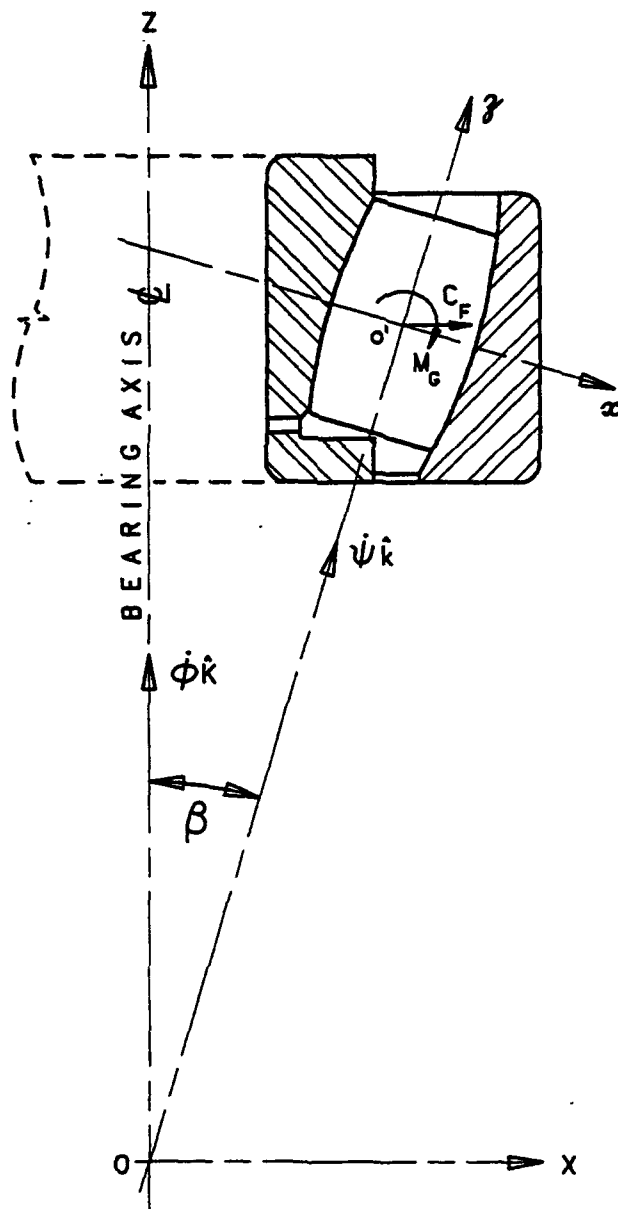


FIGURE 13

## APPENDIX - E

### LOAD-DEFORMATION RELATIONSHIP AND MATERIAL FACTORS

For a cylindrical body of finite length, when pressed onto a plane surfaced body of infinite extension, the normal approach between the axis of the cylinder and a distant point in the supporting body, first presented by Palmgren et. al. [22], is approximately given by,

$$\delta = 4.36E-7[\mathbb{K}^{2.7}Q^{.9}/L^{.8}] \quad (E.1)$$

or

$$\delta = 4.36E-7[\mathbb{K}^{2.7}q^{.9}L^{.1}] \quad (E.2)$$

where  $\mathbb{K}$  is a factor based on the materials of the two contacting bodies and  $Q = qL$  is the total normal force pressing the two bodies together. The material factor  $\mathbb{K}$  is given by,

$$\mathbb{K} = \left[ 1.643E+7 \frac{(\hat{E}_1 + \hat{E}_2)}{\hat{E}_1 \hat{E}_2} \right]^{1/3} \quad (E.3)$$

where,  $\hat{E}_1 = E_1/(1-e_1^2)$  and  $\hat{E}_2 = E_2/(1-e_2^2)$ .

#### (a) RELATIONSHIP FOR STEEL ON STEEL CONTACT:

Let  $E_1 = 29.0E6$  psi,  $E_2 = 29.0E6$  psi,  $e_1 = 0.30$ , and  $e_2 = 0.30$

We get  $\mathbb{K}^{2.7} = 1.0$ . Equation (E.2) then gives us,

$$\delta = 4.36E-7q^{.9}.L^{.1} \quad (E.4)$$

#### (b) RELATIONSHIP FOR CERAMIC ON STEEL CONTACT:

Let  $E_1 = 43.0E6$  psi,  $E_2 = 29.0E6$  psi,  $e_1 = 0.27$ , and  $e_2 = 0.30$

We get  $\mathbb{K}^{2.7} = 0.872$ . Equation (E.2) then gives us,

$$\delta = 3.80E-7.q^{.9}.L^{.1} \quad (E.5)$$

**REPORT DOCUMENTATION PAGE**Form Approved  
OMB No. 0704-0188

Public reporting burden for this collection of information is estimated to average 1 hour per response, including the time for reviewing instructions, searching existing data sources, gathering and maintaining the data needed, and completing and reviewing the collection of information. Send comments regarding this burden estimate or any other aspect of this collection of information, including suggestions for reducing this burden, to Washington Headquarters Services, Directorate for Information Operations and Reports, 1215 Jefferson Davis Highway, Suite 1204, Arlington, VA 22202-4302, and to the Office of Management and Budget, Paperwork Reduction Project (0704-0188), Washington, DC 20503.

<b>1. AGENCY USE ONLY (Leave blank)</b>		<b>2. REPORT DATE</b> September 1993	<b>3. REPORT TYPE AND DATES COVERED</b> Final Contractor Report	
<b>4. TITLE AND SUBTITLE</b> Computer Program for Analysis of High Speed, Single Row, Angular Contact, Spherical Roller Bearing, SASHBEAN Volume II: Mathematical Formulation and Analysis			<b>5. FUNDING NUMBERS</b>  WU-505-63-36 1L162211A47A	
<b>6. AUTHOR(S)</b>  Arun K. Aggarwal				
<b>7. PERFORMING ORGANIZATION NAME(S) AND ADDRESS(ES)</b>  Emerson Power Transmission Corporation McGill Manufacturing Company Valparaiso, Indiana 46383-4299			<b>8. PERFORMING ORGANIZATION REPORT NUMBER</b>  E-8088	
<b>9. SPONSORING/MONITORING AGENCY NAME(S) AND ADDRESS(ES)</b> Vehicle Propulsion Directorate U.S. Army Research Laboratory Cleveland, Ohio 44135-3191 and NASA Lewis Research Center Cleveland, Ohio 44135-3191			<b>10. SPONSORING/MONITORING AGENCY REPORT NUMBER</b>  NASA CR-191182 ARL-CR-81	
<b>11. SUPPLEMENTARY NOTES</b>  Project Manager, Timothy L. Krantz, (216) 433-3580.				
<b>12a. DISTRIBUTION/AVAILABILITY STATEMENT</b>  Unclassified - Unlimited Subject Category 37			<b>12b. DISTRIBUTION CODE</b>	
<b>13. ABSTRACT (Maximum 200 words)</b>  Spherical roller bearings have typically been used in applications with speeds limited to about 5000 r.p.m. and loads limited for operation at less than about 0.25 million DN. However, spherical roller bearings are now being designed for high load and high speed applications including aerospace applications. A computer program, SASHBEAN, has been developed to provide an analytical tool to design, analyze, and predict the performance of high speed, single row, angular contact (including zero contact angle), spherical roller bearings. The material presented in this document is the mathematical formulation and analytical methods used to develop computer program SASHBEAN. For a given set of operating conditions, the program calculates the bearing's ring deflections (axial and radial), roller deflections, contact areas and stresses, depth and magnitude of maximum shear stresses, axial thrust, rolling element and cage rotational speeds, lubrication parameters, fatigue lives, and rates of heat generation. Centrifugal forces and gyroscopic moments are fully considered. The program is also capable of performing steady-state and time-transient thermal analyses of the bearing system.				
<b>14. SUBJECT TERMS</b>  Bearing; Computer aided engineering			<b>15. NUMBER OF PAGES</b> 51	
			<b>16. PRICE CODE</b> A04	
<b>17. SECURITY CLASSIFICATION OF REPORT</b> Unclassified	<b>18. SECURITY CLASSIFICATION OF THIS PAGE</b> Unclassified	<b>19. SECURITY CLASSIFICATION OF ABSTRACT</b>	<b>20. LIMITATION OF ABSTRACT</b>	